COMBINED NSM STEEL BARS AND EXTERNALLY BONDED GFRP IN STRENGTHENING T BEAMS

by

ABDELBASET MAHMOUD TRAPLSI

B.S., Al-Mergab University, Al-Khoms-Libya, 2000

A THESIS

submitted in partial fulfillment of the requirements for the degree

MASTER OF SCIENCE

Department of Civil Engineering
College of Engineering

KANSAS STATE UNIVERSITY
Manhattan, Kansas

2013

Approved by:

Major Professor
Hayder A. Rasheed

Abstract

Nowadays, using the technology of FRP strengthening has become acknowledged by engineers and has reached a full acceptance. However, researchers are always looking for improvement in performance. In this study, external bonding of GFRP and near surface mounting of regular steel bars are combined to improve the behavior, delay the failure and enhance the economy of the strengthening. E-Glass FRP is selected due to its inexpensive cost and non-conductive properties to shield the NSM steel bars from corrosion. On the other hand, the use of NSM bars gives redundancy against vandalism and environmental deterioration of GFRP.

An experimental program was conducted in which four full scale T beams were designed and built. All four specimens were fabricated with Grade 70 steel reinforcement and 8000 psi concrete. Only one beam was loaded beyond first cracking then exposed to highly concentrated deicing salt water to accelerate the corrosion process. All beams were tested by monotonic loading until failure. The load rate was 1 kips/min. The first specimen is tested as a control beam failing at about 15 kips. The second specimen is strengthened using two #5 steel NSM bars and 1 layer of GFRP, both extending to the support. This beam failed at 38.4 kips by GFRP debonding. The third specimen is strengthened with the same system used for the second beam. However, the NSM steel bars were cut short covering only 30% of the shear-span while the GFRP was extended to the support. This beam failed at 25.9 kips by GFRP debonding and NSM delamination due to the lack of sufficient development of the NSM steel bars and the shear stress concentration at the steel bar cut off point. Nevertheless, the fourth beam is strengthened with the same system used for the third beam. The fourth specimen was exposed to severe attack of deicing salt by immersing it in concentrated deicing salt solution for three continuous months. In order to accelerate the corrosion process, the beam was loaded beyond its cracking load before the corrosion procedure. After the completion of the three months, the beam was tested monotonically to failure. It failed at 23.2 kips indicating that some deterioration might have taken place. The failure mode was by GFRP debonding and NSM delamination like the case of Beam 3.However, it was observed after failure that the NSM bars were very well protected by the surrounding epoxy.

Table of Contents

List of Figures

List of Tables

Acknowledgements

This project was made possible by funding from different donators. GFRP strengthening materials were generously donated by VSL Strengthening Products, a division of Structural Group. Steel rebars for construction of the reinforced concrete specimens were donated by Ambassador Steel and Gateway Building Materials.

I would especially like to thank Dr. Hayder Rasheed for the opportunity to participate in this project, and his support during the research. I would also like to thank Dr. Asad Esmaeily, and Dr. Hani Melhem for acting as committee members and providing their support and knowledge in the research. I would thank also Dr. Kyle Riding for providing some consultation regarding the pouring of concrete during cold weather. I would also like to give a special thanks to our Civil Engineering Research Lab Technician, Ryan Benteman for providing assistance in the lab during construction and testing of the experimental specimens. I would also like to thank some of my fellow and former students for providing assistance in the experimental work of the research, especially Augustine Wuertz, Ahmed Al-Rahmani, Narendra Bodapati, Asfandyar Inayat, Mohammed Albahttiti.

CHAPTER 1. INTRODUCTION

1.1. General

Beams are used in all type of structures from buildings to bridges to support slabs. Beams carry slab loads and transfer them to columns or piers. Because of their critical location in the structures, they are subjected to different types of loads (bending, torsion and shear). In terms of cross section shapes, one of the very common types are used in construction are T Beams. This type of cross section gives more flexural resistance because of its geometry which has bigger area at the compression region. Therefore, considerable research work is being performed throughout the world on retrofitting concrete T beams with externally bonded FRP composite materials. In order to investigate, improvements in strength, ductility, and durability, several studies took up concrete T beams retrofitted with carbon fiber reinforced polymer (CFRP) and glass fiber reinforced polymer (GFRP). One of the advantages of using the FRP technique is the ability of continuous usage of the structures or the facilities during the strengthening procedure. FRP composites are lightweight materials which gives numerous advantages over steel such as low self-weight. After about two decades, the outcomes obtained from different investigations regarding improvement in properties like strength/stiffness, ductility and durability of structural members retrofitted with externally bonded FRP composites, shows that there is still room for further improvements. Potentially, this needs additional study in order to investigate FRP composites and find more proper methods to strengthen RC beams.

The use of fiber reinforced polymers (FRP) technology in strengthening has become acknowledged by structural engineers and has reached a full acceptance. Strengthening of Reinforced Concrete (RC) elements by externally bonded (FRP) materials is one of the most widely approved methods for retrofitting existing structures. American national code; ACI Committee 440.2R-08, provisions for the design of elements strengthened with FRP Externally Bonded Reinforcements (EBR) has been in use for some time. However, researchers are always looking for improvement in performance. The technique of using FRP in new concrete structures began with replacement of steel bars with FRP bars. The replacement philosophy was appropriate to avoid corrosion, however, it doesn't utilize the full potential of FRP materials. Several studies showed that the concept of using FRP strengthening to produce composite members was more efficient than replacement of steel bars with FRP bars (Fam and Rizkalla

2002). However, a large number of studies showed premature failures by debonding of the FRP sheets or concrete cover delamination. Usually, the debonding failure occurs within the span at one of the cracks whereas concrete cover delamination starts at the FRP end.

In strengthening for flexural procedure, the FRP reinforcement usually is externally bonded to the tension face of the members with fibers oriented longitudinally along the length of the member to increase the flexural capacity. Even though the advantages of FRP strengthened reinforced concrete (RC) flexural members are desirable, their ultimate failure may occur in a brittle failure mode due to sudden debonding of the FRP system from the concrete or rupture of FRP. Brittle failure mode due to sudden debonding of the FRP is undesirable from the point of view of structural safety. The early FRP debonding failure has been experimentally identified by a number of studies (Sharif et al.1994, Swamy and Mukhopadhaya 1999, Rahimi and Hutchinson 2001). Moreover, using FRP as externally bonded strengthening material leads to thinking about the risk of fire and/or accidental damage. Since that the particular concern is losing the FRP bond, the behavior of structure after losing the FRP needs to sustain the existing loads until the end of the fire time. Therefore, using one of the known techniques of flexural strengthening; Near Service Mounted bars (NSM), could give more sustained capacity in case of fire. Basically, the NSM technique consists of cutting grooves into the concrete cover and bonding rebar to the grooves by using appropriate adhesive material such as epoxy resin or cement mortar. The idea of NSM reinforcement started in Europe by using steel rebar between 1940 and 1950 (Bournas and Triantafillou, 2008).

Corrosion of reinforcing steel is one of the big problems on the US economy, which is very costly, about $297 billion per year, (GangaRao et al. 2001). FRP repair is one of the desirable methods to increase both the strength and durability. Because of its properties such as high strength to weight ratio, resistance to corrosion, and ease of installation, using FRP technique is desirable for deteriorated concrete structure due to exposure to de-icing salts. FRP may provide protection from ingressing salts and other environmental factors by isolating the concrete cover when wrapped around the tension zone. However, there is still a lack of adequate understanding of the long-term performance of Fiber Reinforced Polymer (FRP) composites. GFRP sheets have some desirable properties such as light weight, resistance to salt water attack, deformability and nonconductiveness. GFRP sheets are resistant to chloride and chemical attack (GangaRao et al.

2001). In terms of conductivity, using GFRP sheets as externally bonded reinforcement certainly has an advantage over using CFRP.

The aim of this study is to investigate the behavior of a combination of NSM steel reinforcement and GFRP wrapping of the concrete cover. The second goal is to evaluate the effect of the corrosion exposure.

1.2. Objectives and Scope of the Study

The main objective of this research was to evaluate the behavior of reinforced concrete T beams retrofitted with combining the use of near surface mounted (NSM) steel bars and externally bonded GFRP. To achieve this main objective, several secondary objectives were addressed:

- Study the effect of using full length NSM rebars and shorter NSM rebars and compare them when both beams are strengthened with full length GFRP sheet.
- Having more ductility in the failure mode.
- Study the accelrated short term effect; three months, of deicing salt solution attack on cracked strengthened beam and how behavior differs in case of deterioration.
- Finding the proper method of strengthening by using FRP.
- Recommend some provisions for future research.

1.3. Organization of Thesis

Previous studies on using FRP and NSM bars are presented in Chapter 2. Chapter 2 consists of four parts based on the objectives of this study. Those four parts are flexural strengthening, the effect of adhesive, partially bonded FRP, and durability of externally bonded FRP. Design models relating to the prediction are mentioned as well as their failure modes. The chapter following the literature review is the experimental study. This Chapter explains the design of the laboratory specimens and the properties of the materials that were used to build the specimens. In addition, the description of experimental testing procedures of the specimens, all the steps of construction including making rebare cages, formwork, and casting are mentioned in details in this chapter. Chapter 4 addresses the experimental results and the analysis procedure. This chapter presents the experimental test results which are then analyzed in the same Chapter to determine and explain the effectiveness of combining an externally bonded GFRP and NSM

rebars as an efficient method for reinforcing RC T beams. Chapter 5 has the conclusions are recommendations for future work.

CHAPTER 2. LITERATURE REVIEW

2.1. General

In developed countries, older infrastructure needs to be rehabilitated to make it useable and to extend its service life. Previously, the use of steel plates externally bonded to strengthen RC beams was the state of the art approach. Losing the bond between the corroded steel and concrete was one of the challenges. Moreover, the heavy weight of steel during the installation procedure was another hindering factor. To improve the durability and the constructability of this technique, non-corrosive lightweight materials such as Fiber Reinforced Polymer (FRP) can be a good substitute to steel plates. Design flexibility, improved life cycle cost, high strength, corrosion resistance and weight reduction, are some of the advantages of using FRP reinforcement. [Kalluri 1999]. It has been mentioned by several researchers that the first study to investigate FRP materials for use with reinforced concrete began in Europe in the mid of 1950's [Dhinakaran et al. 2010, Wines et al. 1966, Rubinsky and Rubinsky, 1954]. Based on a research conducted by Meier (1987), the first bonded CFRP concrete repair has been done on site in Switzerland. Nowadays, the use of FRP to strengthen concrete structures has become very popular and wide spread. Another method used to strengthen RC structures is near surface mounting technique (NSM). This technique is not new. The first attempt to use NSM technique was to strengthen a bridge deck slab in the negative moment region in Lapland, Finland in the 1940s. as reported by Soliman et al. 2008.

2.2. Flexural Strengthening

In 1994, Chajes et al. conducted an experimental study to characterize the bond between the composite laminates and concrete. They used carbon fiber reinforced polymer (CFRP) as sheets, strips and plates to strengthen concrete structures. In 1996, they conducted another research study to better understand the bond behavior between the FRP and the concrete surface. In 1996, Hoy et al. investigated fender piles which have FRP casing around a concrete core. These piles showed more capacity in terms of stiffness and strength properties under bending loads [Hoy et al. 1996].

Malek et al. (1998) have conducted an experimental work to predict the failure load of RC beams strengthened with FRP plates due to cover delamination. The study showed a local failure of the concrete cover along the longitudinal reinforcement in the strengthened beams at the termination end of the plate. Grace et al. (1999) studied the performance of RC beams strengthened with CFRP and GFRP sheets and laminates. Their study was conducted to evaluate the influence of the number of layers, epoxy types, and strengthening method. The results showed that all beams failed in a brittle failure mode, with noticeable improvement in strength.

Decker (2007) has conducted an experimental study to confirm that transverse strengthening can control the debonding failure mode. In this study, there were three rectangular reinforced concrete beams and three T beams. The beams were strengthened by using five layers of CFRP. To resist the cover delamination or debonding and allow for a different failure mode, two of the beams were strengthening by using five layers of CFRP wrapped with CFRP U-wraps. This provides flexural anchorage to those beams. The study showed that the beams without U-wraps underwent early separation failure. Whereas, the beams with U-wraps showed that the U-wraps enhance the capacity of the beams and let the FRP reach its full strength and fail in FRP rupture. The increase of the capacity was 220% over the control beam specimens. The specimens were tested in four points bending [Decker 2007, Rasheed et al. 2008]

Castro et al. (2007) performed an extensive experimental study. Twelve T- beams were built and tested to investigate the use of several methods and different materials (CFRP bars, GFRP bars, CFRP strips, CFRP laminates and steel bars). The flexural strengthening systems and the experimental results are shown in table 2-1 below:

Table 2-1:"Flexural Strengthening Systems and the experimental results" [Castro et al., 2007]

Beam	Flexural Strengthening Type	E (GPa)	f'_c (MPa)	$P_{u.theo.}$ (kN)	$P_{u.exp}$ (kN)	$P_{u.exp}$ / $P_{u.theo.}$	Failure Mode
A-1	Control	--	46.3	160	162.6	1.01	Reinforcement yielding
A-2			36.5	156	185.1	1.19	Reinforcement yielding followed by concrete crushing
B-1	3 NSM CFRP strips (2 x 16 mm)	131	49.5	232	245.6	1.06	Peeling off of the CFRP strips and the concrete cover
B-2			52.8	240	250.0	1.05	
C-1	1 NSM CFRP bar (ø10 mm)	147	52.7	225	253.4	1.12	Slipping of the CFRP bar followed by CFRP rupture
C-2			50.1	237	249.6	1.05	
D-1	2 NSM GFRP bars (ø12.7 mm)	40.8	50.1	234	250.0	1.07	Peeling off of the GFRP strengthening together the concrete cover
D-2			35.2	219	226.7	1.04	
E-1	2 layers CFRP sheets (0.0165 x 150 mm)	228	40.0	196	205.7	1.05	Debonding of the CFRP near the support after extensive cracking of the concrete cover below the load point
E-2			47.7	203	215.0	1.06	
F-1	1 steel bar (ø8 mm)	221	35.2	169	198.5	1.18	Reinforcement yielding followed by concrete crushing
F-2			36.4	168	195.4	1.16	

Soliman et al. (2008) conducted an experimental study to investigate the behavior of concrete beams strengthened in flexure with NSM FRP bars. Nine full-scale rectangular concrete beams (3.1 m-long × 200 mm-wide × 300 mm-deep) were tested until failure. The results confirmed that the use of NSM FRP bars is appropriate for strengthening concrete structures. The use of NSM technique increased the load carrying capacity of the tested beams by approximately 100%. However in terms of deflection, beams strengthened with GFRP bars and CFRP bars showed different results. Beams strengthened with GFRP bars had more deflections at failure than those strengthened with CFRP bars.

Rasheed et al. (2010) tested four equivalent composite-based strengthening systems (externally bonded CFRP sheets, externally bonded SRP sheets, NSM prefabricated CFRP strips, and NSM stainless steel bars). Their goal was to achieve about 38% increase in flexural capacity. However, after testing the beams the results showed an increase of approximately 50% in flexural strength in all four beam specimens.

Shit (2011) investigated the flexural behavior of RC T-beams strengthened using (GFRP) by conducting an experimental research. Seven beams including the control one were built and tested to failure. The test method was based on four point bending. The beams were strengthened by using GFRP sheets. The results showed that the most effective reinforcement pattern was the U-wrap GFRP with fibers along the beam axis.

2.3. The Effect of Adhesive Bonding

In 2001, Rahimi and Hutchinson investigated the effect of adhesive bonding on the performance of FRP strengthened beams.. They used three different types of external reinforcement (GFRP, CFRP, and external mild steel). All types of reinforcement were bonded by using a two part epoxy adhesive. The mode of failure depends on the type and thickness of the reinforcement. The beams strengthened with thin laminates failed in a mode of concrete crushing. Whereas, the beams with thicker laminates failed at the end of plates by cover delamination. The failure of the beams reinforced by using external mild steel was steel yielding ultimately followed by plate debonding which occured at the plate ends. The capacity of the beams strengthened by using a composite plate was significantly increased in terms of stiffness and strength over those strengthened with mild steel. The capacity was up to 230% over the control specimen.

Dai et al., (2005) conducted an experimental study to find out the influence of using a normal bonding and flexible bonding systems. Their full-scale test on a 15-m span reinforced concrete bridge T-beam (Figure 2-1) was strengthened using the flexible bonding system and tested to failure. The failure mode was crushing of top flange concrete after steel yields. The ultimate capacity of T-beam was increased at least by 14.6% by the flexible bonding system. The study recommended using the flexible bonding technique for the ultimate limit state strengthening purpose only, which is impractical to implement.

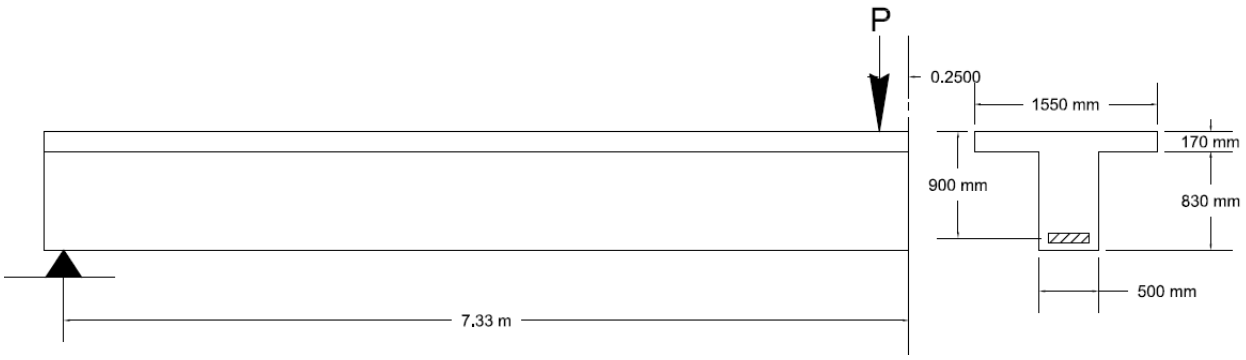

Figure 2-1: Dai et al., (2005), full-scale test on a 15-m span

2.4. Partially Bonded FRP

Choi (2007) developed a new analytical model to study the general behavior of the partially bonded system. The theoretical analysis showed that a partially bonded system has a high prospective to improve deformability without the loss of strength capacity. To verify the analytical model, an experimental program was conducted. A total of seventeen, 3.5m long, RC T-beams were tested. The beams were a mix of externally bonded, near surface mounted, and prestressed NSM. Each group has different unbounded lengths. The study aimed to reach a balance between improvements of load carrying capacity and the corresponding reduction of deformability. The study showed that a classical flexural crack debonding failure was admitted in the fully bonded beams, while it did not occur in the partially bonded beams due to intentional unbonding at mid-span. At the same time, the debonding failure started at the transition point in the partially bonded beams. Table 2 shows the strengthening cases.

Table 2-2 Strengthening Systems adopted by Choi (2007)

Beam Group	Beam No.	Strengthening System	Unbounded length (L_{ub}x2) (mm)
Control	1	--	--
I.	2	Non-prestressed external bonded	Fully bonded
	3	CFRP plate	650x2
	4		850x2
	5		1050x2
II.	6	Non-prestressed NSM CFRP bar	Fully bonded
	7		650x2
	8		750x2
	9		850x2
	10		1050x2
III.	11	Prestressed NSM CFRP bar (40%)	Fully bonded
	12		650x2
	13		850x2
	14		1050x2
	15		1250x2
IV.	16	Prestressed NSM CFRP bar (60%)	Fully bonded
	17		1050x2

2.5. Durability of Externally Bonded FRP

Toutanji and Gomez (1997) studied the long-term durability and effect of harsh environmental conditions. Four types of FRP composite materials were used to strengthen concrete beams including two carbon and two glass materials. The experimental program focused on exposing specimens to wet/dry cycling using salt water on the performance of concrete beams externally bonded with FRP sheets. The results for all specimens unexposed and exposed showed an enhancement in ultimate flexural capacity. Nevertheless, comparing to the control beam the development in ultimate load for the exposed specimens was less than those unexposed. This was because of the deterioration of the bond between concrete and FRP rather than to any degradation of the FRP.

Soudki (2000) has studied the behavior of RC beams strengthened with CFRP laminates subjected to corrosion damage. Ten small-scale beams with cross-sectional dimensions of 4”x6” and a length of 1’-11” were studied in this research (Figure 2-2). The beams were exposed to variable chloride levels (0-3%). Six of the ten specimens were strengthened by externally bonded CFRP laminates to the concrete surface (Figure 2-3). The other four beams were not strengthened. Three of unstrengthened specimens and four strengthened specimens were

subjected to accelerated corrosion procedure by connecting the tensile steel to a constant impressed current (5, 10, and 15% mass loss). The beamss were tested in fixture in a four-point bending.

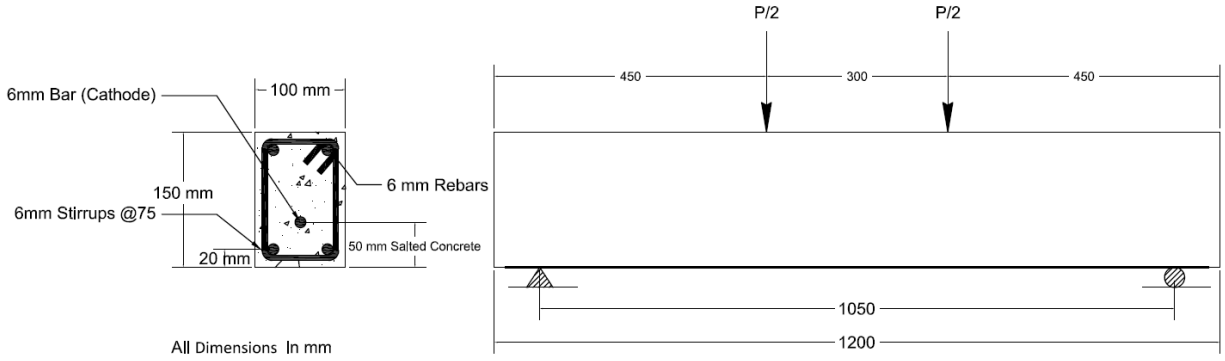

Figure 2-2: Soudki(2000) Test Specimen for Corrosion Without Strengthening.

Test results showed that all strengthened beams positively limited the corrosion cracking. Furthermore, all the strengthened beams showed increased stiffness over the unstrengthened specimens and marked increases in the yield and ultimate strength. The CFRP strengthening scheme was able to sustain and have the same capacity of corrosion damaged concrete beams up to 15% mass loss as the undamaged beams.

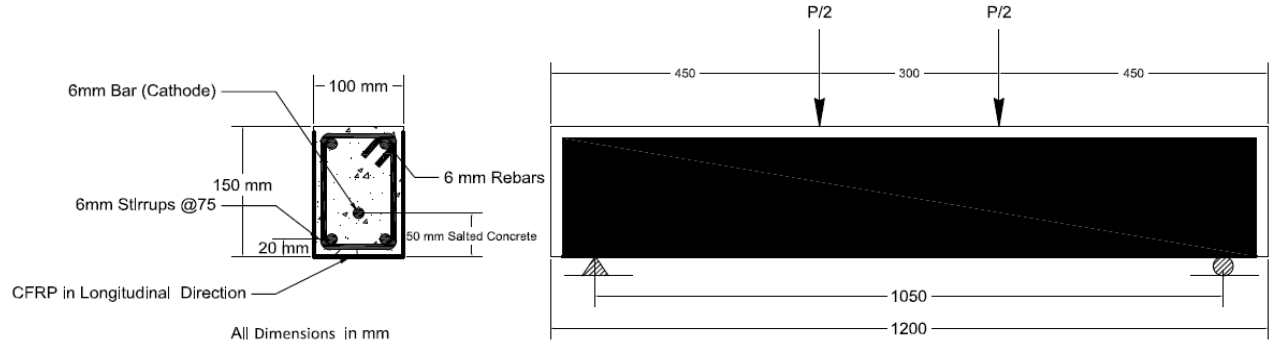

Figure 2-3: Soudki(2000) Test Specimen for Corrosion With Wrappe FRP.

Table 2-3 Summary of Soudki (2000) flexural test results

Category	Unstrengthened Specimens with % Mass loss (0,5,10, and 15)				Strengthened Specimens with % Mass loss (0,5,10, and 15)			
Beam ID	N-0	N-5	N-10	N-15	CF-0	CF-5	CF-10	CF-15
Yield load(kN)	51.7	49	47.3	44.1	62.9	62	58.4	56
% loss in yield strength vs. N-o		5	9	15		1	7	11
ultimate strength (kN)	55.8	51.9	50	47.3		78.7	75.5	72.2
% loss in ultimate strength vs. N-o		7	10	15		4	8	12

In 2008 Parish has conducted a research to study the short- and long-term benefits of concrete rehabilitated with externally bonded (CFRP) sheets. The main objective was to find an efficient way to repair deteriorated concrete bridge girders. The study consisted of 35 RC beam specimens. 14 beams were 6”x 8”x108” and tested on a span of 96”; (Figure 2-4). While, the other 21 beams were 6x8x78” and tested on a span of 72”; (Figure 2-5). In order to accelerate the deterioration, the beams were built by using chloride contaminated, low strength and highly porous concrete. Also, electric current technique was used to achieve early deterioration; (Figure 2-6). The specimens were tested at ages of 28 days, 8 weeks, 25 weeks, 40 weeks, and 66 weeks. Two Different Substrate Repair Techniques were used. The first method was done by keeping the old deteriorated concrete and none of the old concrete was removed prior to FRP repair. While, the other method was performed by removing the old concrete and replacing it with high strength polymer concrete containing corrosion inhibitors (Figures 2-7,8,9 and 10).

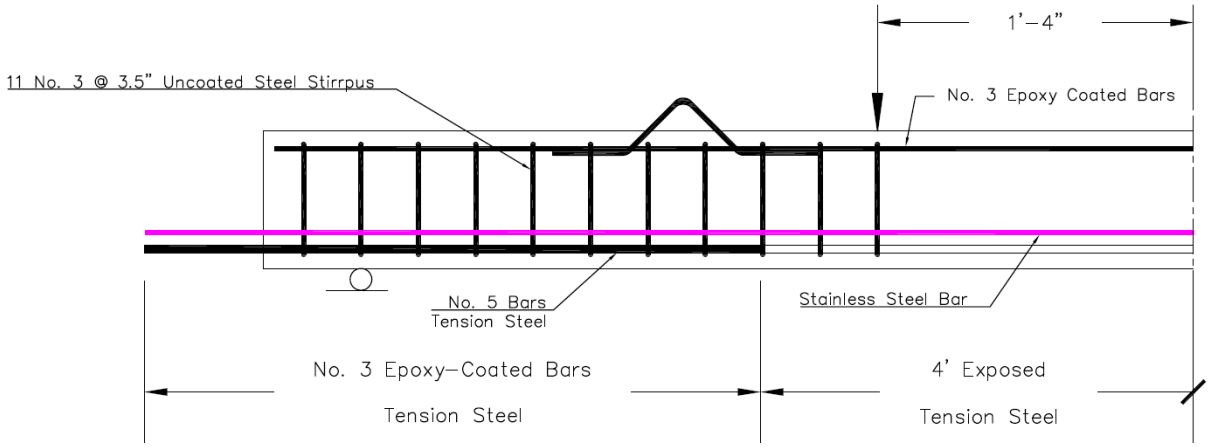

Figure 2-4: Parish (2008), Part I Beam Specimen (Reinforcement Diagram)

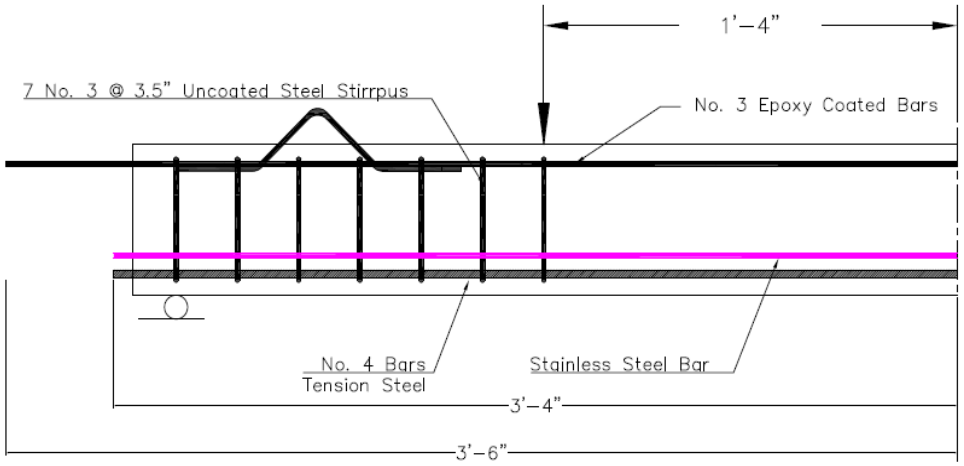

Figure 2-5: Parish (2008), Part II Beam Specimen (Reinforcement Diagram)

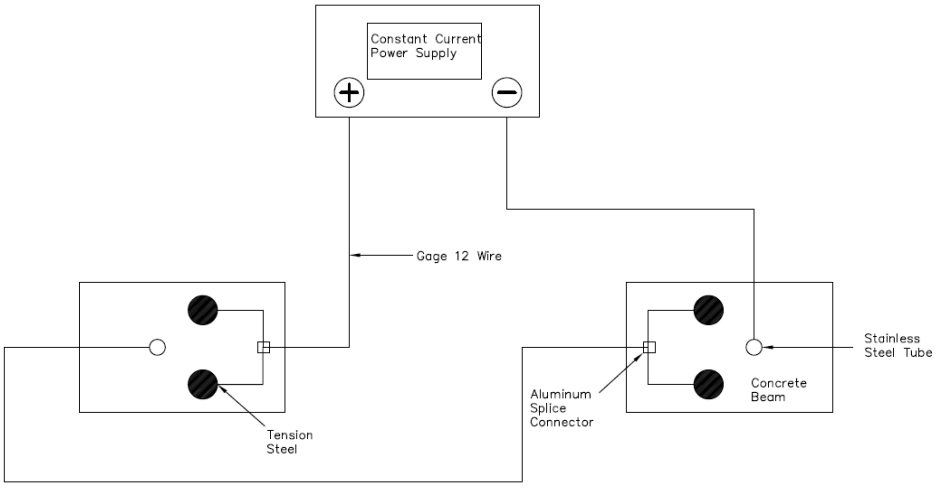

Figure 2-6: Parish (2008), Wiring Scheme for Accelerated Aging via Induced Electric Current.

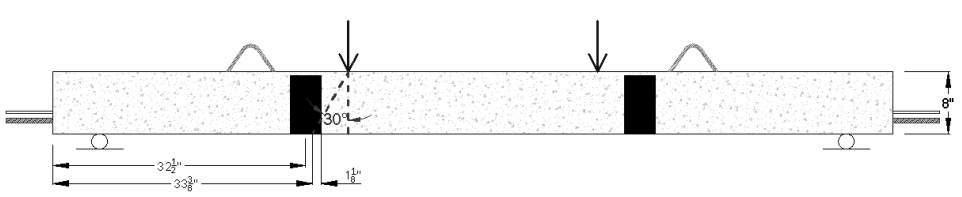

Figure 2-7: Parish (2008), Part I FRP Wrapping Scheme I

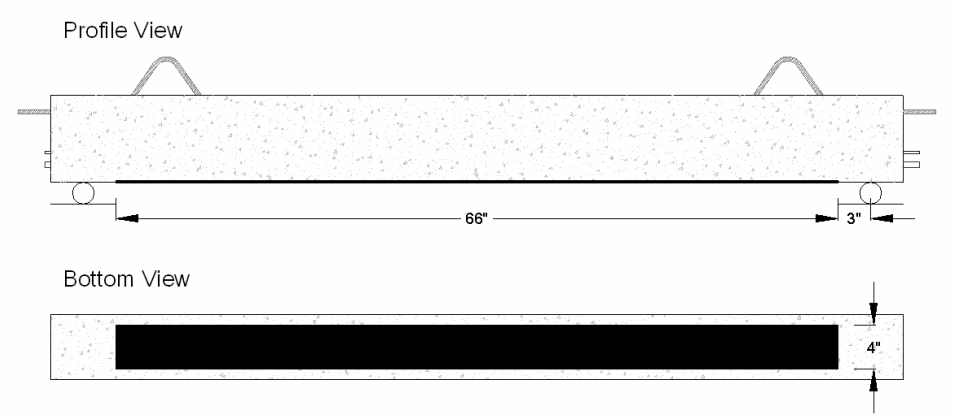

Figure 2-8: Parish (2008), Parish, Part II FRP Strengthening Scheme I

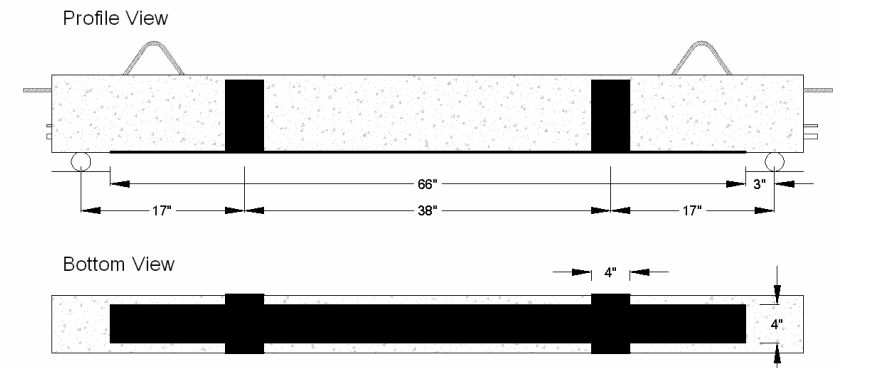

Figure 2-9: Parish (2008), Part II FRP Strengthening/Wrapping Scheme II

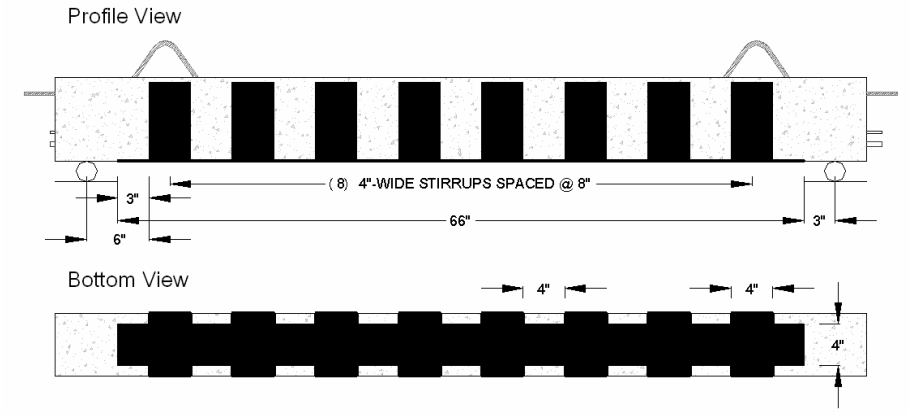

Figure 2-10: Parish (2008), Part II FRP Strengthening/Wrapping III

CHAPTER 3. EXPERIMENTAL STUDY

3.1. Materials

The materials of the present experimental program are concrete, steel reinforcing bars and GFRP sheets. Their mechanical properties have been provided by the manufactures. Nevertheless, all the materials were tested consisting of tensile tests for both the longitudinal and transverse steel reinforcement as well as the GFRP coupons and compression tests for the concrete 4x8" cylinders.

3.1.1. Concrete

The concrete that was used in casting of the four beams is composed of Portland cement Type I, water, sand, gravel, and crushed stone delivered by a ready mix company on 1/24/2012. The mix design nominal strength was 8000 psi. Sixteen cylinders (4in. x 8in) were taken for the actual material testing on beam test dates. The first set of 4 cylinders was tested on 02/21/2012 the same day the control T beam (T1) was tested. All cylinders were cured at the moisture room except 4 cylinders were left outside where the beam were located to see the effect of the low temperature on the compressive strength. The last set of cylinders was tested on 11/19/2012. Table 3.1 shows the results of the average compressive strength f'c of each beam (Figure3-1).

Figure 3-1: Casting of Concrete Cylinders.

Table 3: Compression Strength

CYLINDER	LOAD	COMPRESSIVE STRENGTH f'c (psi)	DATE
C1- outside with no cure	97185	7733	2/21/2012
W1- cured at moisture room	103160	8209	
W2- cured at moisture room	97915	7791	
W3- cured at moisture room	100915	8030	
C2- outside with no cure	95720	7572	6/22/2012
W4- cured at moisture room	104895	8335	
W5- cured at moisture room	105245	8377	
W6- cured at moisture room	102220	7694	
C3- outside with no cure	105246	8376	7/5/2012
W7- cured at moisture room	104896	8344	
W8- cured at moisture room	111546	8873	
W9- cured at moisture room	104880	8342	
C4- outside with no cure	118160	9400	11/19/2012
W10- cured at moisture room	113460	9033	
W11- cured at moisture room	120910	9622	
W12- cured at moisture room	119151	9490	

Before the casting started, both slump test and air content were measured. The slump test was 2'' (The slump test was performed based on ASTM C143 / C143M - 10a) and the air content 4.5 % (The air content test was performed based on ASTM C231 / C231M – 10). During the casting, concrete power vibrator was used to avoid any undesirable air voids left in concrete, which was efficiently used for quality control purpose. Since that the casting was during winter session, the temperature at the daytime was around 40° F and it reaches lower than 26° F during the night. In order to avoid any freezing effects during the setting time, the concrete mix had an accelerator admixture (Calcium Chloride) to reduce the setting time. After finishing the concrete surface, another additional procedure to avoid any freezing through at the first 12 hours was covering the specimens with black plastic blanket to restore the heat and have fast curing (Figure3-2,3) .

Figure 3-2: Casting of the Concrete T-Specimens.

Figure 3-3: Curing of the Concrete by Covering with Plastic Blanket.

3.1.2. Steel Reinforcement

All the steel rebar in tension region including NSM bars consisted of deformed No.5 reinforcing bars while No.3 hanger bars were used as compression steel for fabricating the steel cage. The steel stirrups also consisted of deformed No.3 steel bar. The material properties of both rebars No.3 and No.5 were provided by the manufacturer to have a modulus of 29000 ksi (200,000 MPa) and yield strength of 70 ksi (483 MPa). The steel rebar used to construct the four beams was donated by Ambassador Steel Inc. out of Kansas City, MO. Figure 3-4 shows the reinforcement details used for the beams.

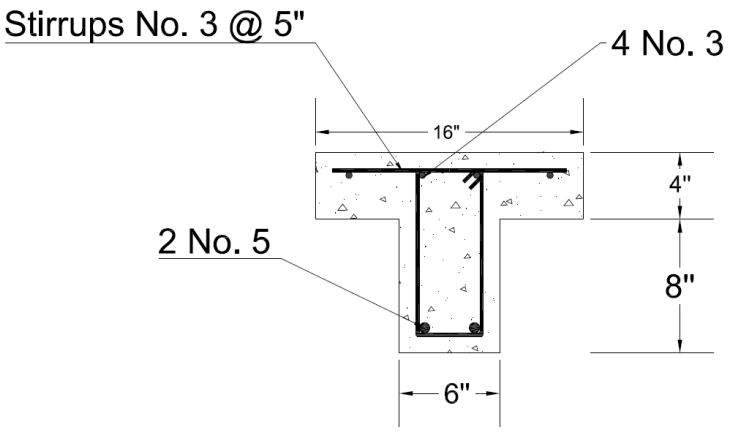

Figure 3-4: Beam Specimen Cross Section

3.1.3. Glass Fiber Reinforced Polymer (GFRP)

The epoxy resin and GFRP materials were all donated by VSL Industries (Baltimore, MD). Based on the tensile test that was performed in mechanical engineering department lab at Kansas State University, following the standard tensile test according to ASTM D3039, the Glass Fiber Reinforced Polymer (GFRP) had an average modulus of 2,168 ksi and an average ultimate tensile strength of 38,400psi. These values correspond to an average ultimate strain of 0.0177. The test had six specimens. Three specimens were made by only one layer while the other three specimens were made of two layers (Figure3-5). However, the manufactures mechanical properties were higher. The modulus of elasticity was 3,030 ksi while the ultimate tensile strength was 66,720 psi which corresponds with an ultimate strain of 0.022. These properties correspond to a thickness of 0.05" as reported by the manufacture. Table 3-1 shows the mechanical properties of GFRP as tested by the mechanical engineering lab.

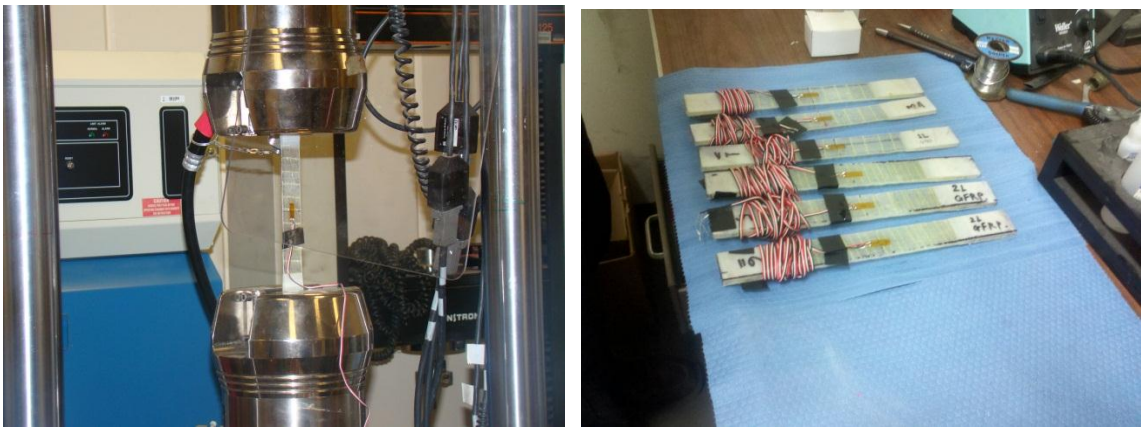

Figure 3-5: GFRP Tensile Test According to ASTM D3039.

Table 3-1: Shows the Stress vs. Strain of GFRP

Specimen	Width	Average Thickness	Ultimate Strength (ksi)	Modulus(ksi)	Ultimate Strain (με)
GFRP-1	1.00	0.099	32.7	2173	15065
GFRP-2	1.00	0.103	32.7	1971	16598
GFRP-3	1.00	0.111	31.9	1886	16936
GFRP-4	1.00	0.166	44.5	2026	21954
GFRP-5	1.00	0.142	38.5	2265	16987
GFRP-6	1.00	0.152	50.2	2688	18675
Average GFRP	-	-	38.4	2168	17702

3.2. Construction of Test Specimens

3.2.1. Design of Specimen Geometry

The design was based on an analysis software which is a nonlinear beam analysis program developed by Calvin Reed, a previous graduate student of Kansas State University. Figure 3-6 shows the experimental test setup with total lengths of 16 feet and a clear span length of 15.5 feet. The length was selected based on the length of previous test specimens examined by Brandon Decker (2007); a former graduate student of Kansas State University, to study the effect of CFRP anchorage on the strengthened beam capacity. Each T-beam specimen was built with a flange width of 16 in., a flange thickness of 4 in. The full depth of the section was 12 in. with a web width of 6 in. The dimensions of the cross sections are shown in (figure 3-4).

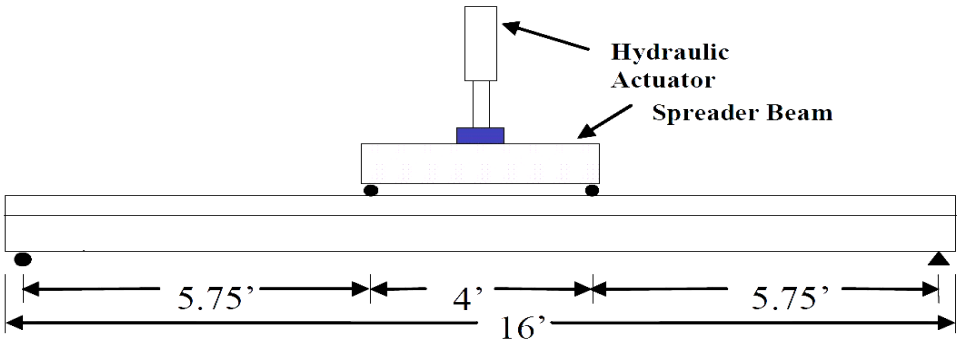

Figure 3-6: Testing Setup of the Beams

Four beams were built with the same reinforcement details and different strengthening schemes. The first beam (T1) was the control beam which has neither GFRP sheets nor NSM bars (Figure 3-7). Beam T2 was strengthened by using one layer of externally bonded GFRP sheet wrapped around the tension zone 5" up the sides and extending to the support with full length of two #5 NSM bars at the bottom cover (Figure 3-8,9). The other two beams (T3&T4)

were strengthened by using short NSM bars (7.5 ft. length) with one layer of externally bonded GFRP sheet wrapped the tension zone 5" up the sides and extending to the support (Figure 3-10). Beam T4 was prepared to be tested for flexural purpose with no corrosion while beam T3 was prepared to be tested after exposure it to highly concentrated deicing salt water solution (25% concentrated by weight). The beam was loaded up to exceed the crack load (5 kips) for five cycles to make sure that it had some propagated cracks.

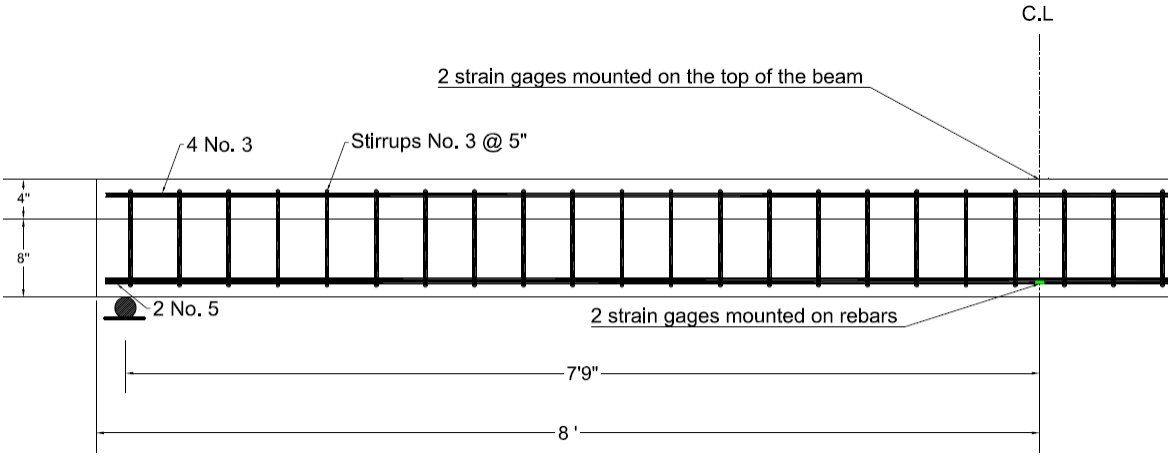

Figure 3-7: Reinforcement Details of the Control Beam T1.

The primary tension reinforcement was composed of two steel rebars with #5 diameter of rebar. The longitudinal compression reinforcement consisted of 4 rebars with a #3 diameter of rebar. These were connected transversely by 14in long #3 rebars spaced every 5in spaced every 5in The shear reinforcement was made of #3 rebars spaced every 5 in. on center. Concrete cover was 1in in all sides. In Figure 3-8 below, an illustration of the cross section is given for beams T2, T3 and T4.

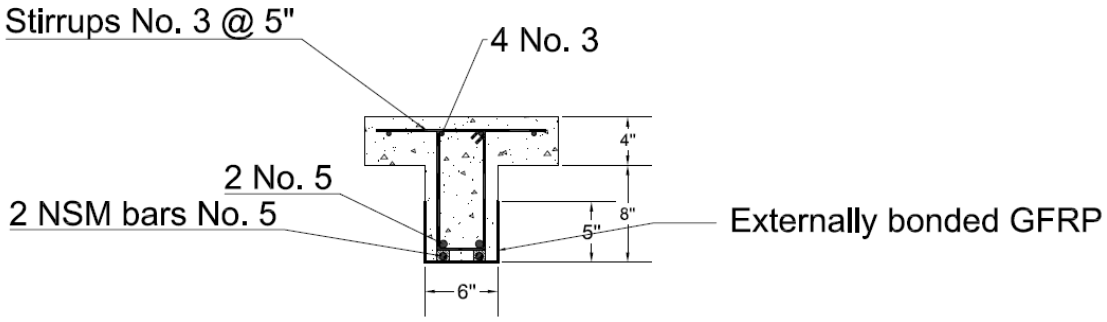

Figure 3-8: Beam Specimen Cross Section.

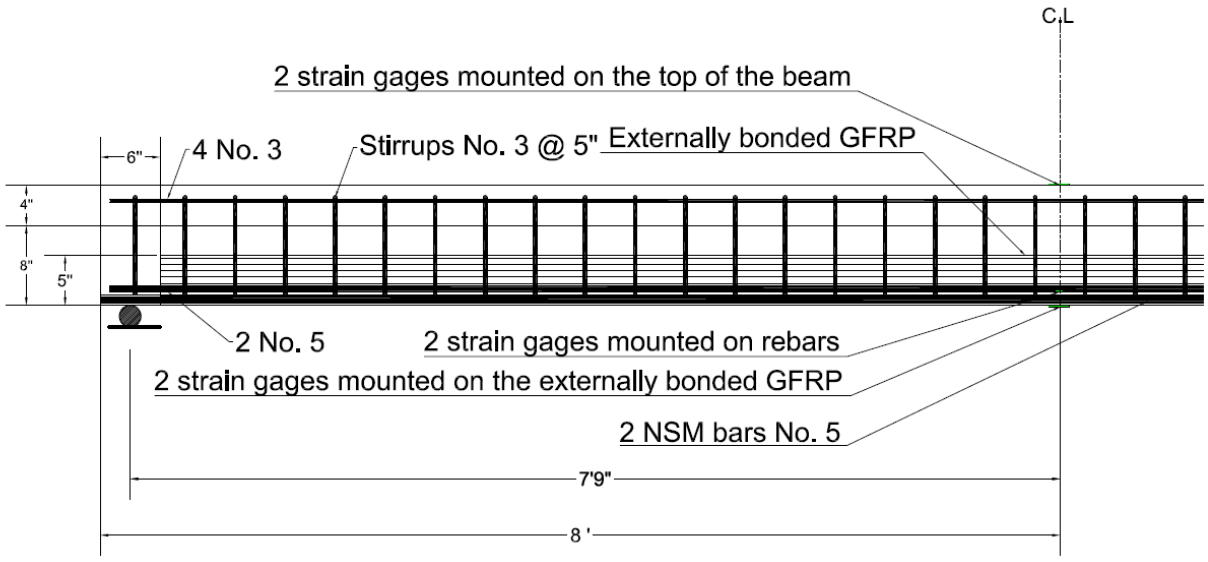

Figure 3-9: Reinforcement Details of Beam T2 (Full Length NSM Bars + Externally Bonded GFRP).

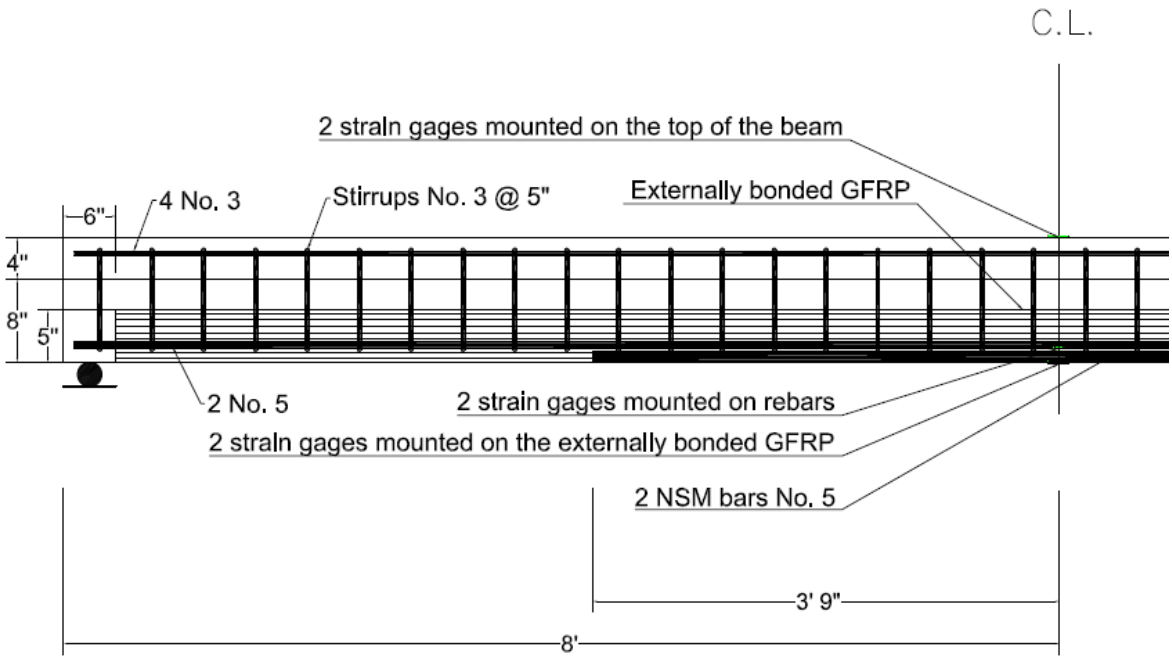

Figure 3-10: Reinforcement Details of Beam T3&T4 (7.5' Length NSM Bars + Externally Bonded GFRP).

3.2.2. Formwork

Formworks consisting of plywood boards and lumber planks were built for casting in order to achieve the similar dimensions for each beam. The assembly of all wooden formwork and steel rebar caging was done in the Civil Engineering department wood and steel shop. The forms had to be assembled in two halves then combined to create a 16 ft long form. After the individual components of lumber and plywood are cut to their dimensions, they are assembled outside behind the lab in the area of concrete casting. Wooden grooves were premade by nailing two pieces of lumber (1"x1") in the bottom face of the formwork (Figure 3-11). Then, the wooden grooves were hand chiseled out of the beams. Figure 3.12 shows the top view of the formwork with reinforcement cages in-place for specimen casting. The formwork was properly oiled before casting. Two formworks were used to cast two beams at a time. Wooden form offered flexibility in terms of adjusting the flange width due to its lightweight. In order to increase the bond between the adhesive and the concrete, the grooves, the bottom and sides of the beams were sand blasted to remove any additional wood, dirt, or undesirable material such as large "bug holes" or deformations. Bug holes or deformations were filled in with epoxy to create an even surface to apply the GFRP sheets

Figure 3-11: Top view of the Formwork Place for T-Specimen Casting.

Figure 3-12: Top View of the Formwork with Reinforcement Cages In-Place for T-Specimen Casting.

3.2.3. The Assembly of the Rebar Cage

The longitudinal steel was cut to its length by the manufacturer. The steel stirrups for transverse reinforcement were bent to the required dimensions manually. The longitudinal reinforcement and the stirrups were assembled by using rebar ties. Figure 3-13 shows the finished rebar cage used for the rectangular part of the T shaped beams. To record the strain change during the testing process, two strain gages were mounted on both main tension rebars to be embedded in the beams before the casting. Then, the strain gages were protected by using duct tape. ½" diameter plastic hose was used to protect the strain gages wires (Figure3-14, 15). To let the beams easy to move and handle, two hocks were made by using #5 rebar in each beam, which were embedded and extended to the top out of the beam (Figure 3-16). 1" rebar chairs were tied to the bottom and sides of the cages to adjust the cage to its position in the formwork. Figure 3-16 shows the rebar cage inserted into the formwork and prepared for casting.

Figure 3-13: The Finished Rebar Cage Used for the Rectangular Part of The T Shaped Beams.

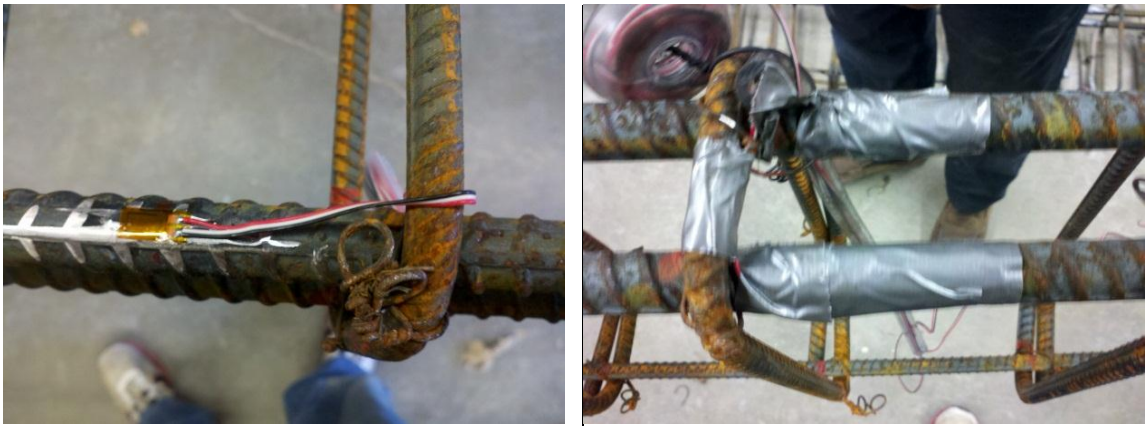

Figure 3-14: Strain Gages on Rebar.

Figure 3-15: The Strain Gage Wire Protected by a Plastic Hose.

Figure 3-16: The Rebar Cages Inserted Into the Formwork and Prepared for Casting.

3.3. Strengthening of Beams

3.3.1. Installing of NSM bars

The first step was installing the NSM bars. The grooves were hand chiseled out of the beams and then the sides of the grooves were sand blasted to remove any additional wood, dirt, or undesirable material (Figure 3-17). The NSM steel rebars were cut to size and placed into the grooves. This procedure was performed by applying epoxy in the grooves until they were more than half-way full. The rebars were pushed into the epoxy and the excess epoxy was scraped off. Figure 3-18 and 3-19 shows the process of applying the epoxy into the grooves.

Figure 3-17: Getting the Wooden Pieces of Lumber Out of the Grooves.

Figure 3-18: Procedure of Applying Epoxy Into the Grooves.

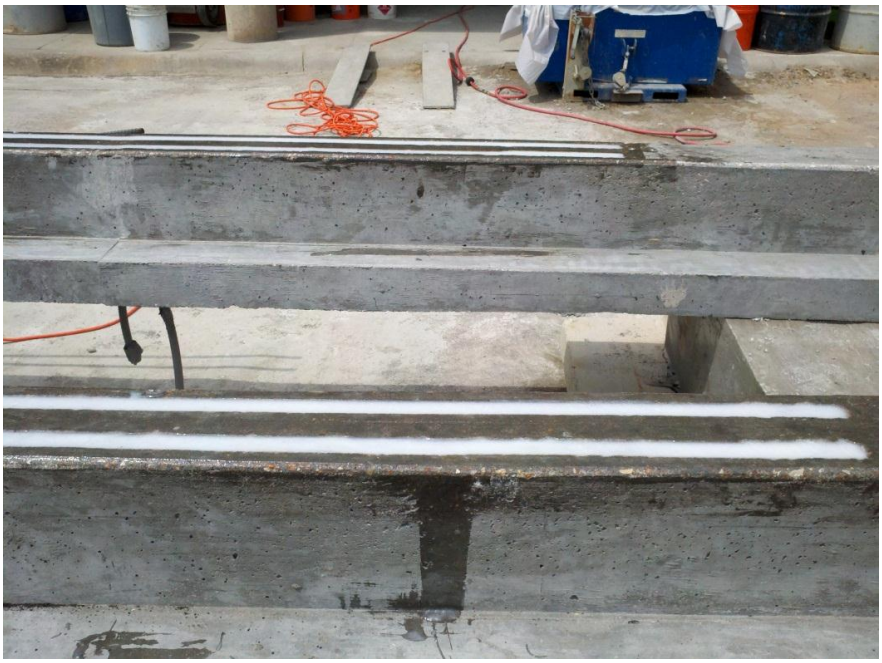

Figure 3-19: NSM Bars inside the Grooves Covered with Epoxy.

3.3.2. Surface Preparation

In order to have efficient bond and avoid premature failure debonding, the surface of the concrete had to be adequately cleaned and roughened. The surface was sandblasted until it had a roughenrd finish and then cleaned with an air blower to remove all dirt and debris. The ACI 440.2R-08 requires making the corners of the beams rounded. Grinder was used to round off the corners. Figure 3-20 shows the process of sandblasting the beams [VSL, PART I, 2012]. Figure 3-21 shows a picture of sandblasted vs. smooth surface.

Figure 3-20 : Beam Sandblasting Process.

Figure 3-21: In the Top is Sandblasted Surface; In the Bottom is Unsandblasted Surface.

3.3.3. Application of GFRP

Following the surface preparation, the second step was applying the GFRP sheets. In order to avoid weather conditions that might be harmful to the process of applying the FRP sheets, the beams were taken inside. The resin was mixed and applied on the beam surface (Figure 3-22). Then the GFRP sheet was placed on top of the epoxy resin coating and the resin is squeezed through the flattening of the fabric with the roller. Air bubbles entrapped at the epoxy/concrete or epoxy/fabric interface are eliminated (Figure 3-23, 24) [VSL, PART II, 2012].

Figure 3-22: Epoxy Mix and Applying Procedure.


Figure 3-23: Installing the FRP Sheets.

Figure 3-24: Applying the Epoxy Resin Coating with the Roller.

3.3.4. Corrosion Procedure

One of the specimens was exposed to a highly corrosive concentrated salt water solution by submerging the tension side in it. The most common deicing salt (Sodium Chloride) was used and dissolved in tap water. The percentage of salt to water was 25% by weight (Figure 3-25). Wooden box was assembled in a size that lets the web part of the T beam be immersed in the salt water. Two layers of plastic sheets were used to isolate the wooden box. Both sides of the wooden box were extended ten inches to monitor the water level in the immerse tub. The specimen was loaded beyond the crack load up to 5k for five cycles in order to accelerate the

corrosion process. The beam was exposed to salt water for three months then tested as the other by monotonic loading to failure. However, the strain gages were not mounted neither on FRP or concrete top side until the corrosion exposure period was over and the beam was dried up.

Figure 3-25: Dissolving Deicing Salt in Tap Water.

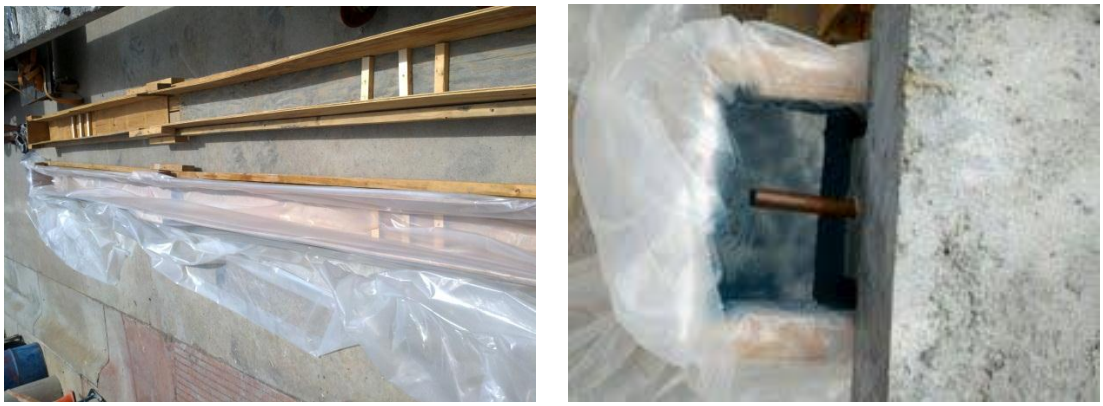

Figure 3-26: Wooden Box Insulated by Plastic Sheets to Immerse Specimen T3.

3.3.5. Experimental Setup

The T-beams were tested in the loading frame of the structural engineering laboratory of Kansas State University, Manhattan, KS. The testing procedure for all the specimens was similar. All the beams were cured for a period of 28 days then its surface is prepared by using sandblasting. The two-point loading method is used for testing beams with a uniform moment region. This has the advantage of having a pure flexure between the two points. Two-point loading is conveniently provided by the arrangement shown in Figure3-27.

The load is transferred through a hydraulic loading system and connected to a spreader beam. The spreader beam is put on rollers seated on steel plates bonded on the test member with hydrocal cement in order to provide a smooth leveled surface. The test specimen has two supports bonded by using a similar procedure to that of the spreader plates. The specimen is

placed over the two supports leaving 3in from the ends of the beam making the clear span equal to 15.5ft. The remaining 15.5ft are divided into three parts as shown in the Figure3-27. Two LVDT (Linear variable differential transducer) sensors are used for recording the deflection in both sides of the midspan (Figure3-28).

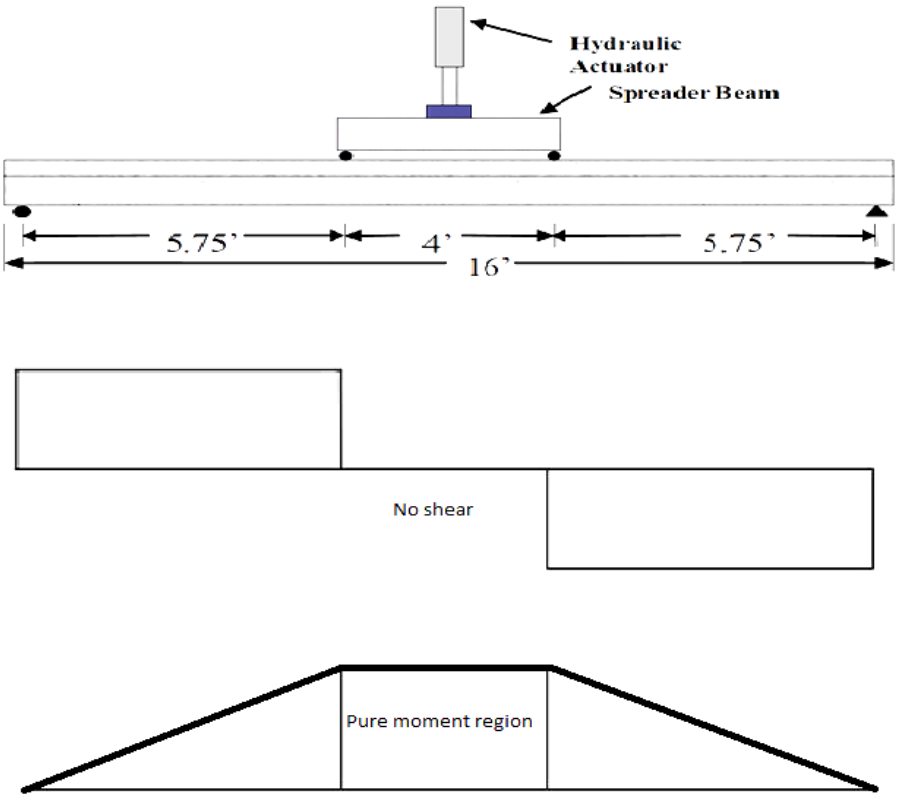

Figure 3-27: Force, Shear and Bending Moment Diagram for Two Points Loading.

Figure 3-28: Two LVDTs Are Used For Recording the Deflection in Both Sides of the Beam Midspan.

Three several types of strain gages are mounted in each beam based on material surface (concrete, steel, and FRP). The control beam had four strain gages. Two gages are located on the upper face of the T-section to monitor strain at concrete upper face (Figure 3-29). The other two gages are mounted on the tension rebars to monitor strain at tension steel (Figure 3-30). In addition to those two types of strain gages, two other strain gages were mounted to measure the strain at the bottom on the GFRP laminates (Figure 3-31).

Figure 3-29: Two Strain Gages at Concrete Upper Face.

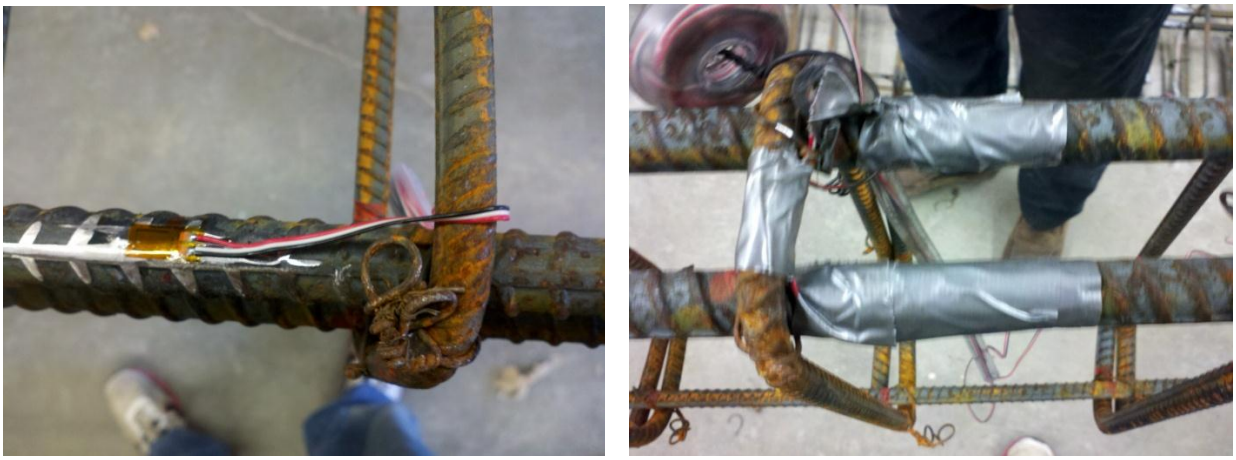

Figure 3-30: Two Strain Gages at Steel Rebars.

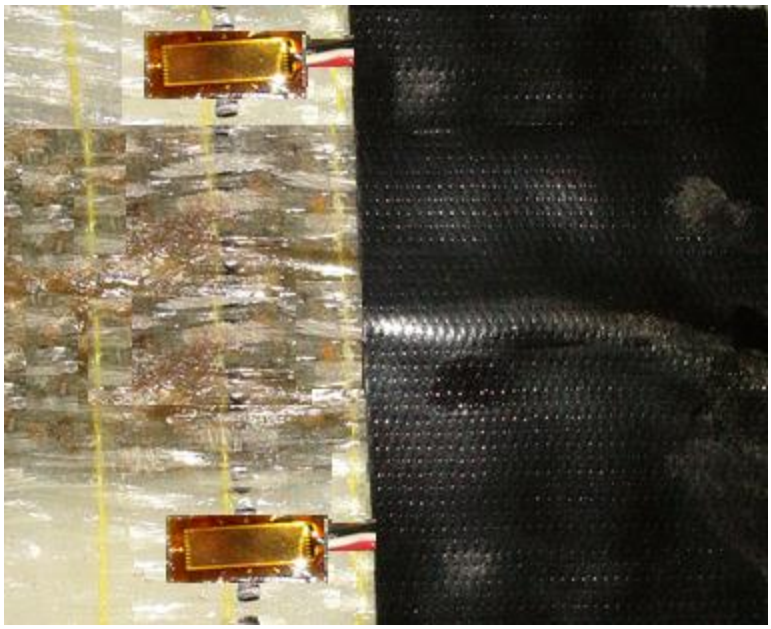

Figure 3-31: Two Strain Gages at Steel Rebars.

CHAPTER 4. RESULTS AND ANALYSIS

4.1. Analysis Program

Microsoft Excel analysis program software was used to design the lab specimens. The software was devolved by Calvin Reed, a previous graduate student of Kansas State University. The software is designed in a way that it gives the user the choice of assiging one of two cross sections (T beam, Rectangular beam). The analysis method of the software was a nonlinear beam analysis. Geometries, material properties or loading types are reachable and adjustable. The program also gives the option to choose the type of reinforcement, whether it is mild steel, prestressed, glass bars or FRP sheets. The program also allows users to reach macro code and adjust the outcome. After the specimens were built the actual dimensions were used to predict the analytical ultimate load, stresses and strains. The program predicts the flexural response of the specimen by using strain compatibility based on the specimen geometry and material properties.

4.2. Analysis and Results

4.2.1. Beam T1 (Control)

From this analysis, the ultimate moment capacity of 38.39 kip-ft is expected. This capacity is reached by an ultimate load of 12.15 kips with a maximum deflection of 6.88 inches. The beam T1 was tested as control beam. It was set up prior to testing on 2/21/2012 (Figure 4-1). The beam was loaded in load control at a rate of 1 kip/minute. The control system is designed to capture the correct peak load. Figure 4-2 shows the beam at maximum deflection before the failure happened.

The test results showed that the beam failed at a load of 15.4 kips. The difference between the theoretical value and the experimental value is 3.25 kips. The difference comes from the fact that the analysis assumes elastic-perfectly plastic steel behavior while the steel in the experiment underwent strain hardening response. However, it is obvious from Figure 4-4 that the yielding load of the analytical response was slightly higher than the experimental yielding load. At the failure load, the deflection at midspan was 6.7 inches and the failure mode of the control beam was a ductile concrete crushing of the beam (concrete crushing failure after yielding of the

main tension steel) (Figure 4-5). Table 4-1 shows a summary of the results of the control beam. From Figure 4-6 it can be seen that the analytical ultimate steel strain, which was predicted by the program, was higher than the experimental ultimate strain since the strain gage seems to have gone bad right after first yielding. Figure 4-4, 5, 6 show comparisons of analytical and experimental response for specimen T1.

Table 4-1: Summary of Experimental Results for Beams T1.

Specimen	Ultimate Load (Kips)	Ultimate Steel Strain	Deflection (In)	Ultimate Load Increase	Failure Mode
Analysis	12.15	0.0454	6.88	N.A.	Concrete Crushing
Experimental	15.40	0.0053	6.70	3.25	Concrete Crushing

Figure 4-1: Control Beam T1 before Testing.

Figure 4-2: Beam T1 Just Prior to Failure.

Figure 4-3: Beam T1 after Concrete Crushing Failure.

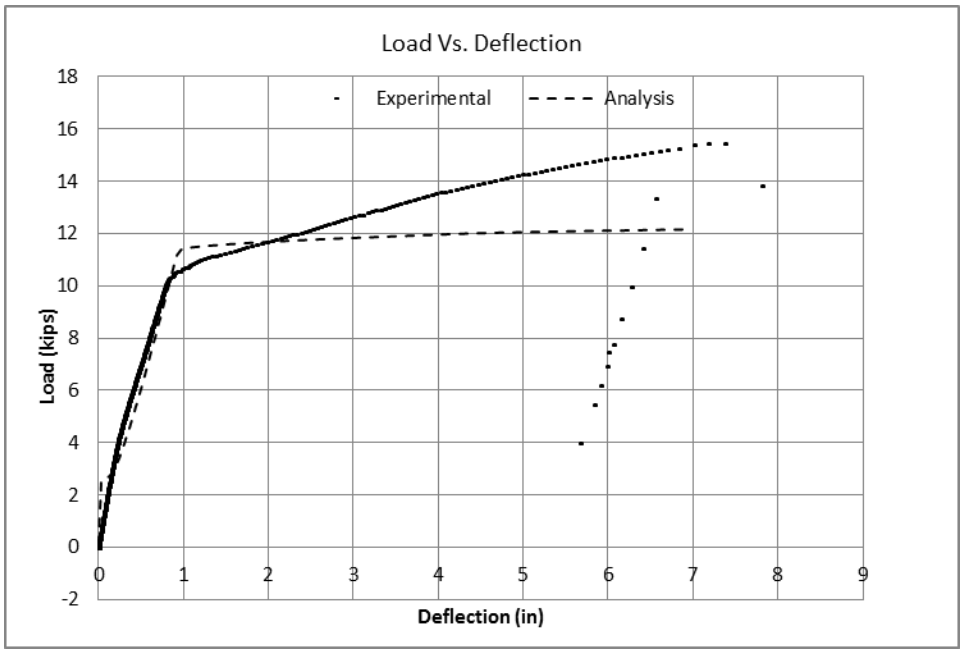

Figure 4-4: Comparison of Analytical and Experimental Load vs. Deflection for Specimen-T1.

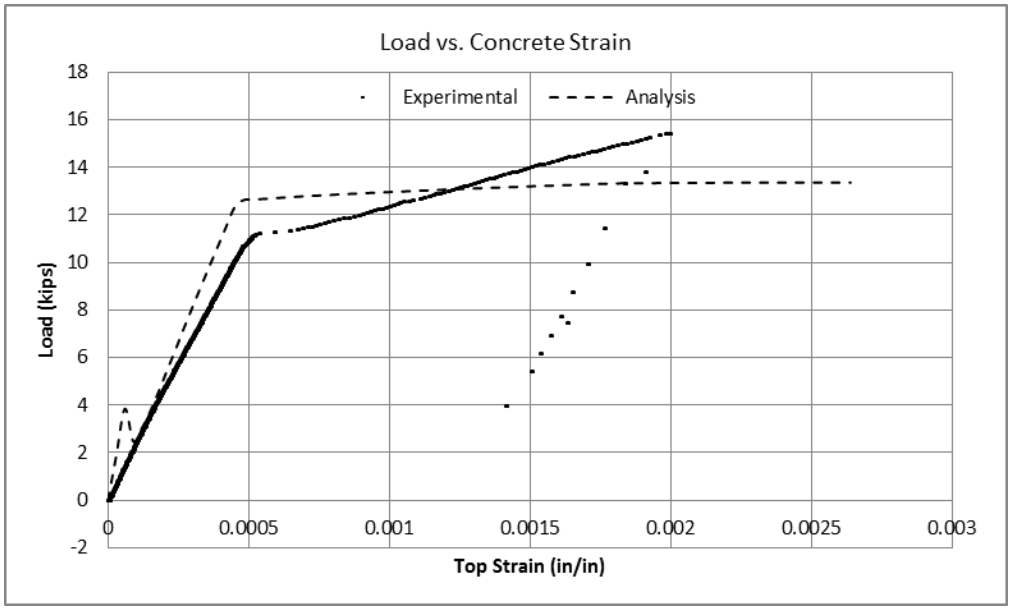

Figure 4-5: Comparison of Analytical and Experimental Top Concrete Strain for Specimen-T1.

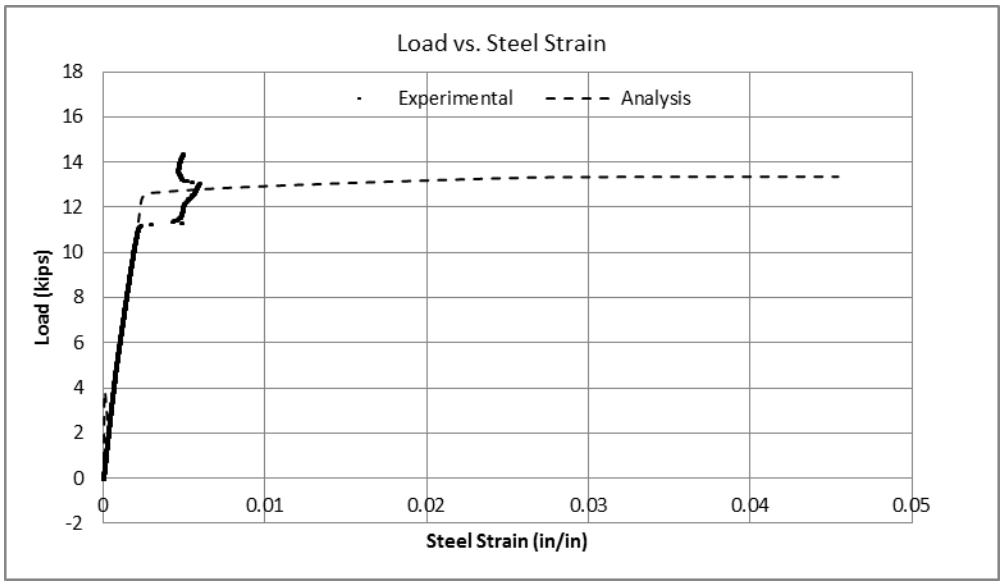

Figure 4-6: Comparison of Analytical and Experimental Rebar Strain for Specimen-T1.

4.2.2. Beam T2 (strengthened by GFRP laminates with Full length of NSM bars)

The second beam was built to investigate the effect of combined NSM bars and externally bonded FRP. It was strengthened by two full length#5 NSM bars and GFRP laminates. The beam was set up prior to testing on 6/22/2012 (Figure 4-7). It was loaded in load control at similar rate as the control beam's rate which is 1 kips/minute. From the analysis, the ultimate moment capacity was relatively high (98.83 kip-ft). This capacity is reached by an ultimate load of 34.87 kips with a maximum deflection of 4.29 inches. However, the test results showed a significant improvement in flexural capacity. The experimental ultimate load value was more than the analytical value. The beam failed at a load of 38.4 kips with a maximum deflection very close to the predicted value (4.01 inches). Figure 4-12 shows that the yielding load of the experimental was about to be equal to the analytical yielding load.

Table 4-2: Summary of Experimental Results for Beams T2.

Specimen	Ultimate Load (Kips)	Ultimate GFRP Strain	Ultimate Steel Strain	Deflection (In)	Ultimate Load Increase (kips)	Failure Mode
Analysis	34.87	0.0179	0.0149	4.29	N.A.	Cover Delamination
Experimental	38.43	0.00646	0.00133	4.01	3.65	Cover Delamination

Table 4-2 shows the summary of the results of beam T2. The analytical ultimate steel strain, which was predicted by the program, was higher than the experimental ultimate strain again due to the early failure of the strain gage. By looking at figure 4-10, it is noticeable that the experimental curve shows more ductility than it was expected. Thus, the failure was more ductile and improved compared to typical failure with FRP. Figure 4-11, 12 and 13 show comparisons of analytical and experimental respones for specimen T2.

Figure 4-7: Beam T2 with Full Length of NSM Bars before Testing.

Figure 4-8: Cover Delamination Failure followed by GFRP Debonding.

Figure 4-9: Shows the Yielding of Compression Steel at the Flange of Beam T2.

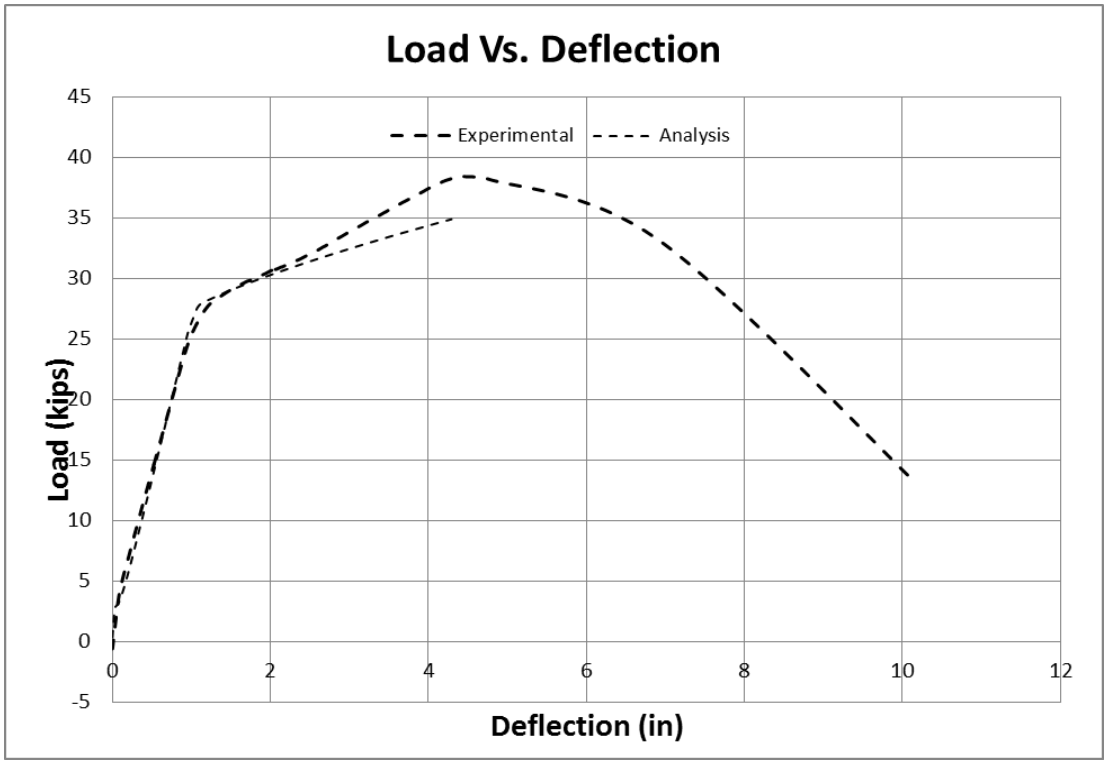

Figure 4-10: Comparison of Analytical and Experimental Load vs. Deflection for Specimen-T2.

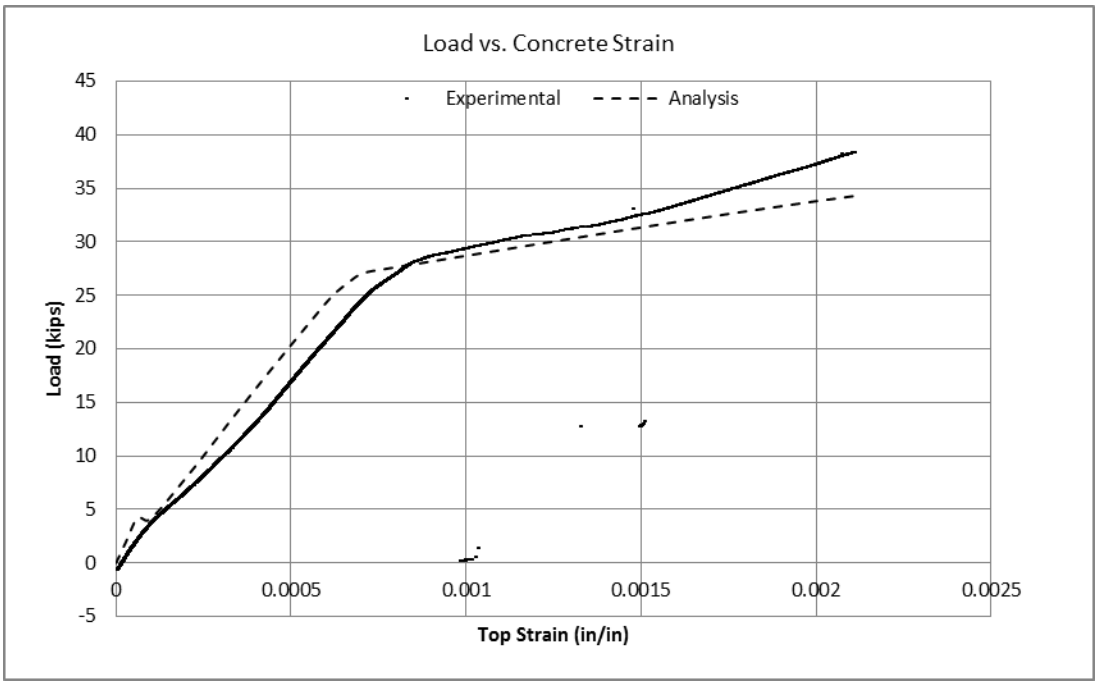

Figure 4-11: Comparison of Analytical and Experimental Top Concrete Strain for Specimen-T2.

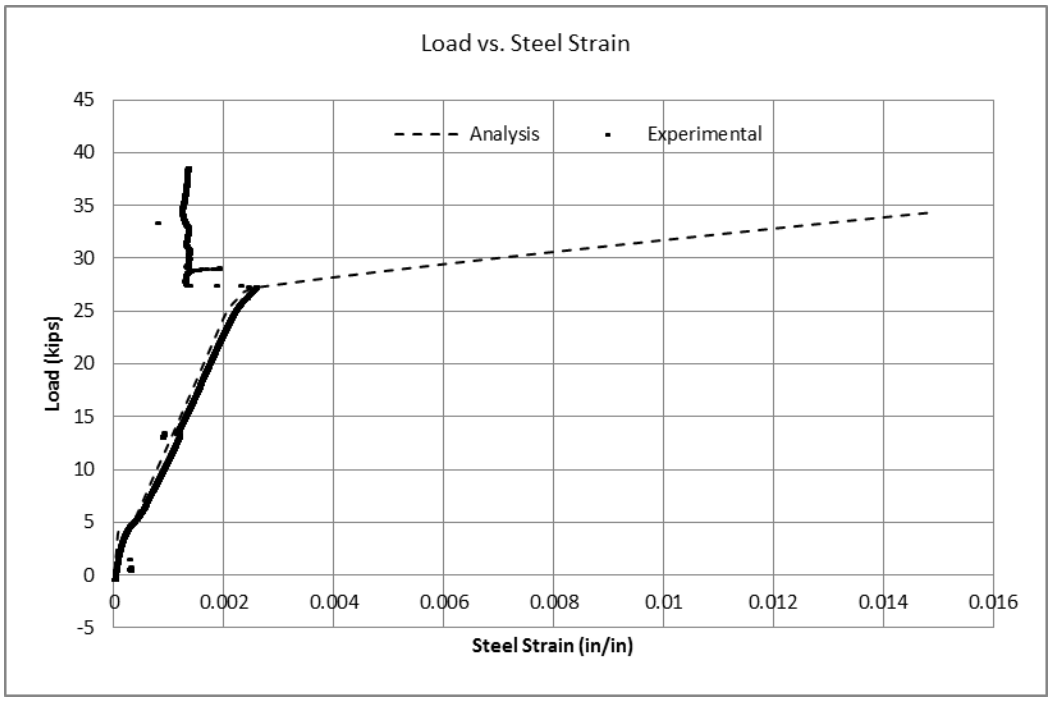

Figure 4-12: Comparison of Analytical and Experimental Rebar Strain for Specimen-T2.

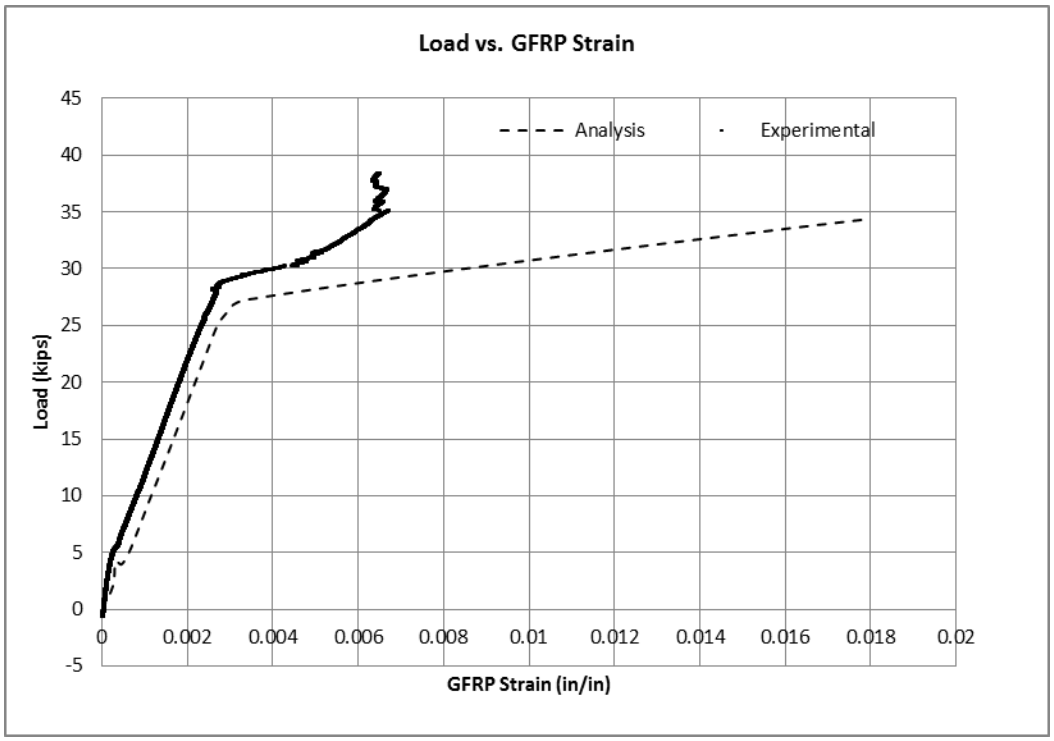

Figure 4-13: Comparison of Analytical and Experimental GFRP Strain for Specimen-T2.

4.2.3. Beam T3 (for corrosion test purpose with short NSM bars)

The third beam was built to study the effect of corrosion on a beam that was strengthened with combination of NSM bars and GFRP laminates. It was strengthened by two 7.5' length #5NSM steel rebars and one layer of GFRP laminates. The beam was submerged in highly concentrated deicing salt solution for three month after been loaded above the cracking load for five cycles. This procedure yielded some signs of corrosion on the uncovered part of the beam web. Figures 4-14 and 15 show some red stains of rusted steel at the edge of FRP.

Figure 4-14: Some Red Stains at Beam T3 After Submerging in Deicing Salt Water.

Figure 4-15: Some Red Stains at the End.

The beam was set up prior to testing on 11/19/2012 (Figure 4-16). From the analysis, the ultimate moment capacity was relatively high (99.33 kip-ft). This capacity corresponded with an ultimate load of 33.36 kips and a maximum deflection of 4.31 inches. Although the test results showed an improvement in flexural capacity, it was less than that was anticipated. The short development length of NSM bars affected the flexural capacity negatively.

Figure 4-16: Beam T3 before Testing.

From Figure 4- 18, it is noticeable that the NSM bars were pushed at their ends causing an early debonding of GFRP. The premature was failure attributed to the concentration of shear stresses at the end of NSM bars. The experimental ultimate load value was less than the analytical value. This was anticipated to the fact that the analysis could not capture the short

NSM development length. The beam failed at a load of 23.14 kips with a maximum deflection at the peak load that was relatively small (1.36 inches) and less than the predicted value (4.31 inches). Figure 4-17 shows that the yielding load of the experimental curve was slightly smaller than the analytical yielding load.

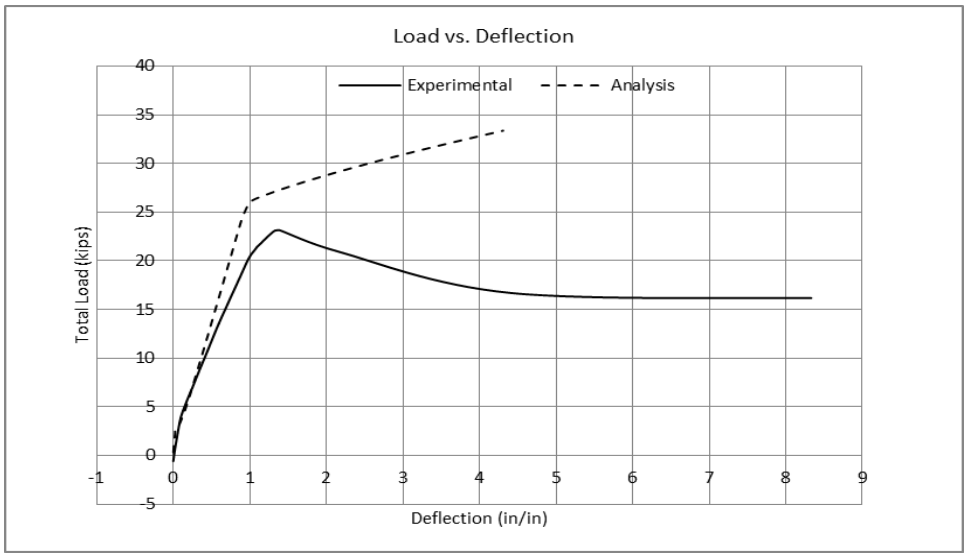

Figure 4-17: Comparison of Analytical and Experimental Load vs. Deflection for Specimen-T3.

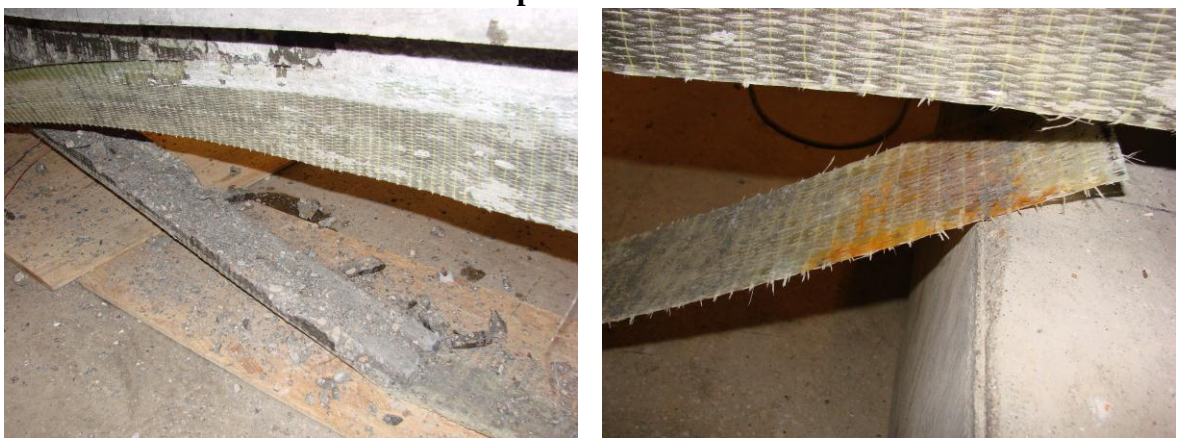

Figure 4-18: Cover Delamination Failure Followed by GFRP Debonding in T3.

Table 4-3: Summary of Experimental Results for Beam T3

Specimen	Ultimate Load (Kips)	Ultimate GFRP Strain	Ultimate Steel Strain	Deflection (In)	Failure Mode
Analysis	34.87	0.017824	0.01514	4.31	Cover Delamination
Experimental	23.14	0.00646	0.00133	1.36	Cover Delamination

Table 4-3 shows the summary of the results of beam T3. The analytical ultimate steel strain, which was predicted by the program, was higher than the experimental ultimate strain. By looking at figure 4-17, it noticeable that the experimental curve shows more ductility than it was expected. However, there was a decline in load with the ductility. Figure 4-19, 20, and 21 shows comparison of analytical and experimental for specimen T3.

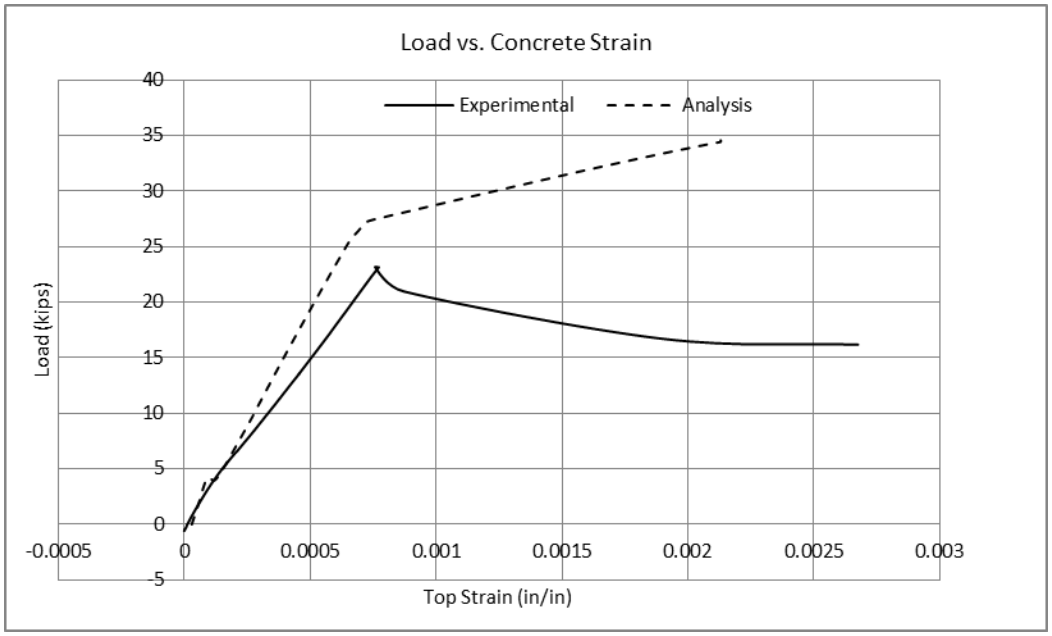

Figure 4-19: Comparison of Analytical and Experimental Top Concrete Strain for Specimen-T3.

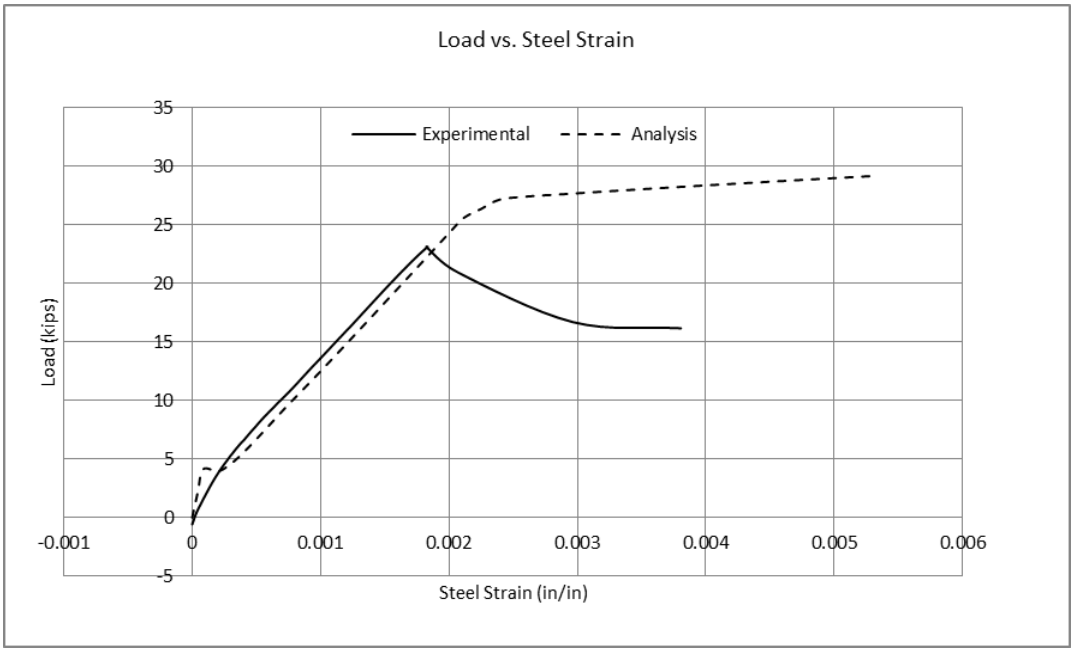

Figure 4-20: Comparison of Analytical and Experimental Rebar Strain for Specimen-T3.

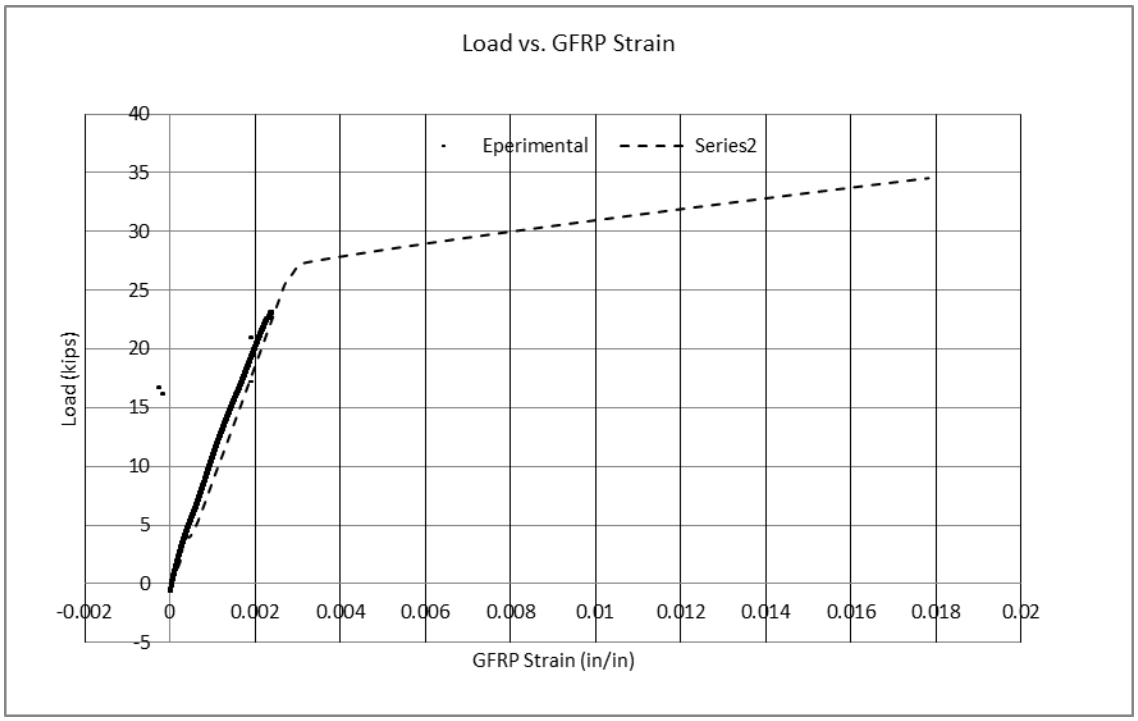

Figure 4-21: Comparison of Analytical and Experimental GFRP Strain for Specimen-T3.

The results showed that the difference between the ultimate load of the beam exposed to corrosion and the unexposed beam was not big. This means that the exposed beam could sustain and fail at an ultimate load very close to the unexposed beam. Looking at Figure 4-22, it is obvious that the epoxy along with the GFRP jacket could protect the NSM steel rebars from corrosion. There was no sign of rusted steel at the NSM bars.

Figure 4-22: Failure of Beam T3

4.2.4. Beam T4 (with short NSM bars)

The fourth beam was prepared to study the effect of short development length of NSM steel bars. It was strengthened by two 7.5' length #5 NSM bars and one layer of GFRP laminates as done with the third beam. The reason was to compare the result of beam T4 with beam T3 which was built to examine the corrosion effects. The beam was set up prior to testing on 7/5/2012 (Figures 4-23).

Figure 4-23: Beam T4 before the Testing.

Even though the design of beam T4 was similar to the design of beam T3, the analysis results were slightly different because of the actual beams dimensions were measured after concrete hardening and considered in the actual calculation. From the analysis, the ultimate moment capacity was also relatively high (98.31 kip-ft). This capacity is corresponded with an ultimate load of 32.97 kips and a maximum deflection of 4.28 inches. Although, the analysis results showed an improvement in flexural capacity, the shortening of the length of NSM bars affected the flexural capacity negatively. The development length of the 7.5 ft NSM steel bars was insufficient and caused a relatively premature failure due to stress concentrations at the edge of the rebar (Figure 4-24).

Figure 4-24: Premature Failure Due to Stresses Concentrations at the End of the Rebar in Beam T4.

Figure 4-25: Premature Cover Delamination Failure Followed with GFRP Debonding of Beam T4.

The results showed that the difference between the ultimate load of beam T4 and control beam was considerable. The beam failed at 25.93 kips. The ultimate load increased by 168.37%. From Figure 4-26 , it can be seen that both carves of analysis and experimental were combatable until the yielding point then the beam started to fail which means that the NSM steel bars cussed a premature failure and the NSM steel did not reach the ultimate load that has been predicted by the analysis program. While the predicted maximum deflection was 4.28 inches, the experimental maximum deflection was only 1.55 inches at the point of the peak load. Table 4-4 shows the comparison of key experimental and analytical data points for beam T4. It is evident from Figure 4-27, 28 and 29 that all strain gages stopped functioning at the first yielding in the beam.

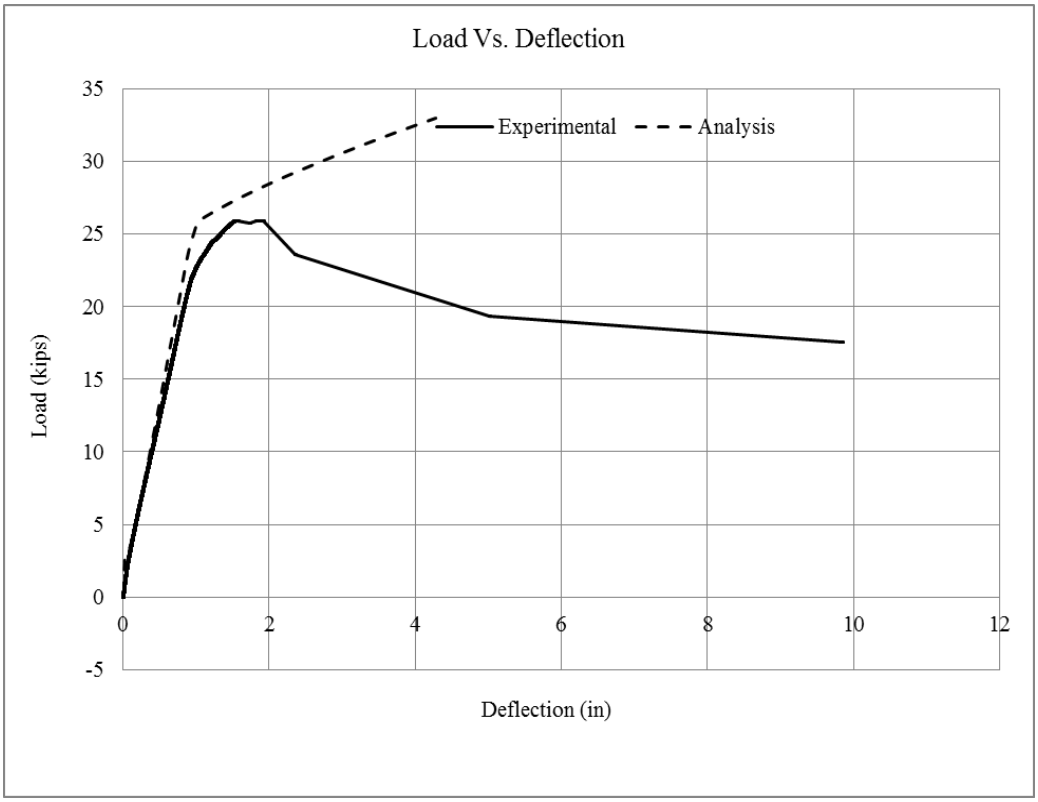

Figure 4-26: Comparison of Analytical and Experimental Load vs. Deflection for Specimen-T4.

Table 4-4: Summary of Results of Beam T4.

Specimen	Ultimate Load (Kips)	Ultimate GFRP Strain	Ultimate Steel Strain	Deflection (In)	Failure Mode
Analysis	32.97	0.01770	0.01463	4.28	Cover Delamination
Experimental	25.93	0.00197	0.00230	1.55	Cover Delamination

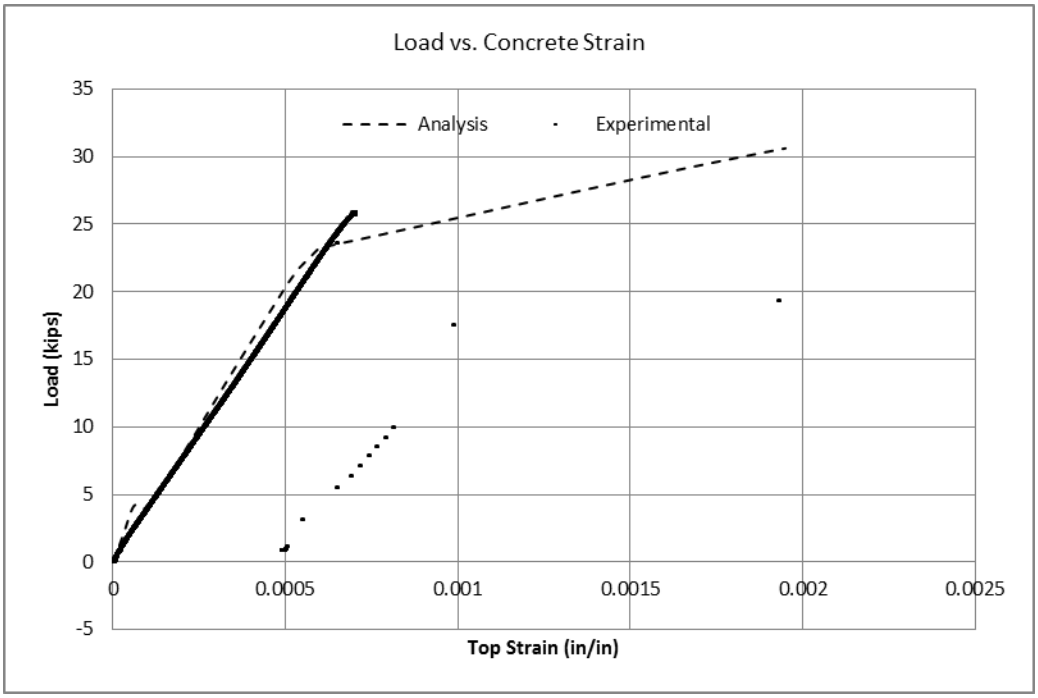

Figure 4-27: Comparison of Analytical and Experimental Top Concrete Strain for Specimen-T4.

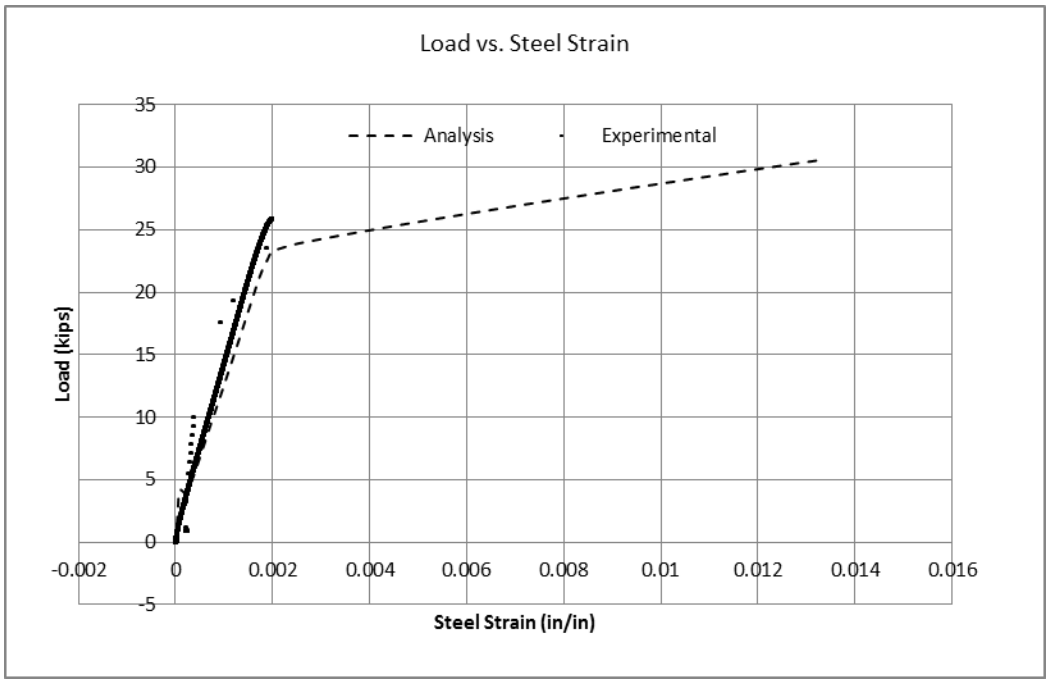

Figure 4-28: Comparison of Analytical and Experimental Rebar Strain for Specimen-T4.

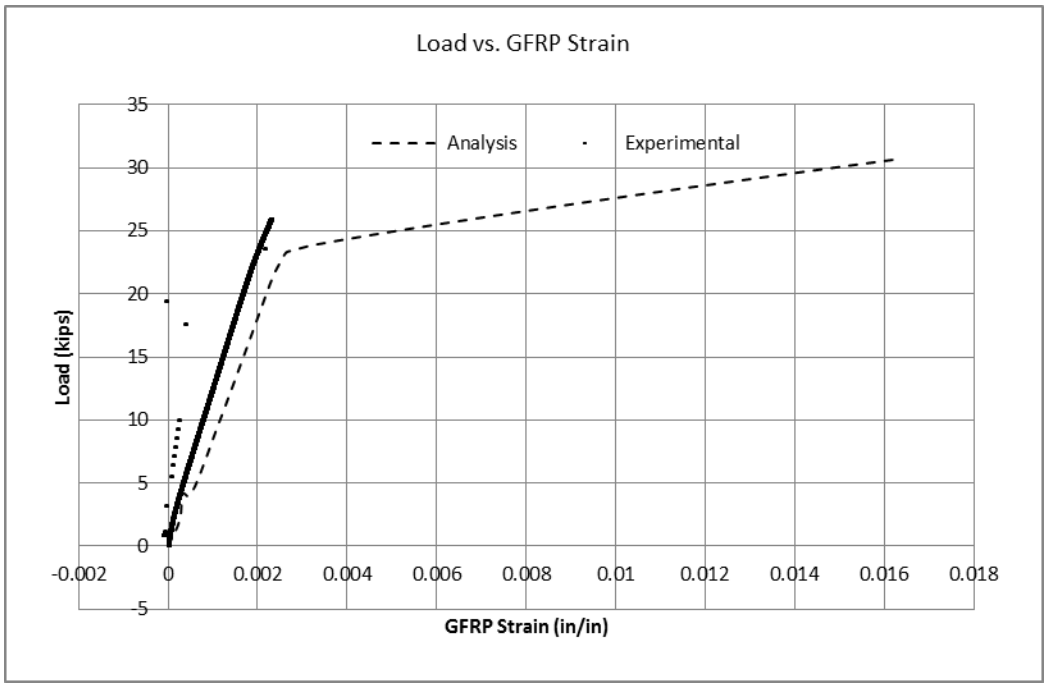

Figure 4-29: Comparison of Analytical and Experimental GFRP Strain for Specimen-T4.

4.3. Summary of Results

Table 4-5 shows a comparison of ultimate load and ultimate deflection for all specimens. From figure 4-30, it is obvious that beam T2 had the highest ultimate load and a desirable mode failure.

Table 4-5: Summary of Results of All Studied Beams.

Specimen	Ultimate Load (kips)	Deflection (in.)	Load Increase (%)	Failure Mode
Beam T1 (Control)	15.4	6.70	N/A	Concrete Crushing
Beam T2 (Full Length NSM Reinforcement + GFRP)	38.43	4.01	249.54	Cover Delamination
Beam T3 (7.5 ft. NSM Reinforcement + GFRP) For Corrosion Purpose	23.14	1.36	150.26	Cover Delamination
Beam T4 (7.5 ft. NSM Reinforcement + GFRP)	25.93	1.55	168.37	Cover Delamination

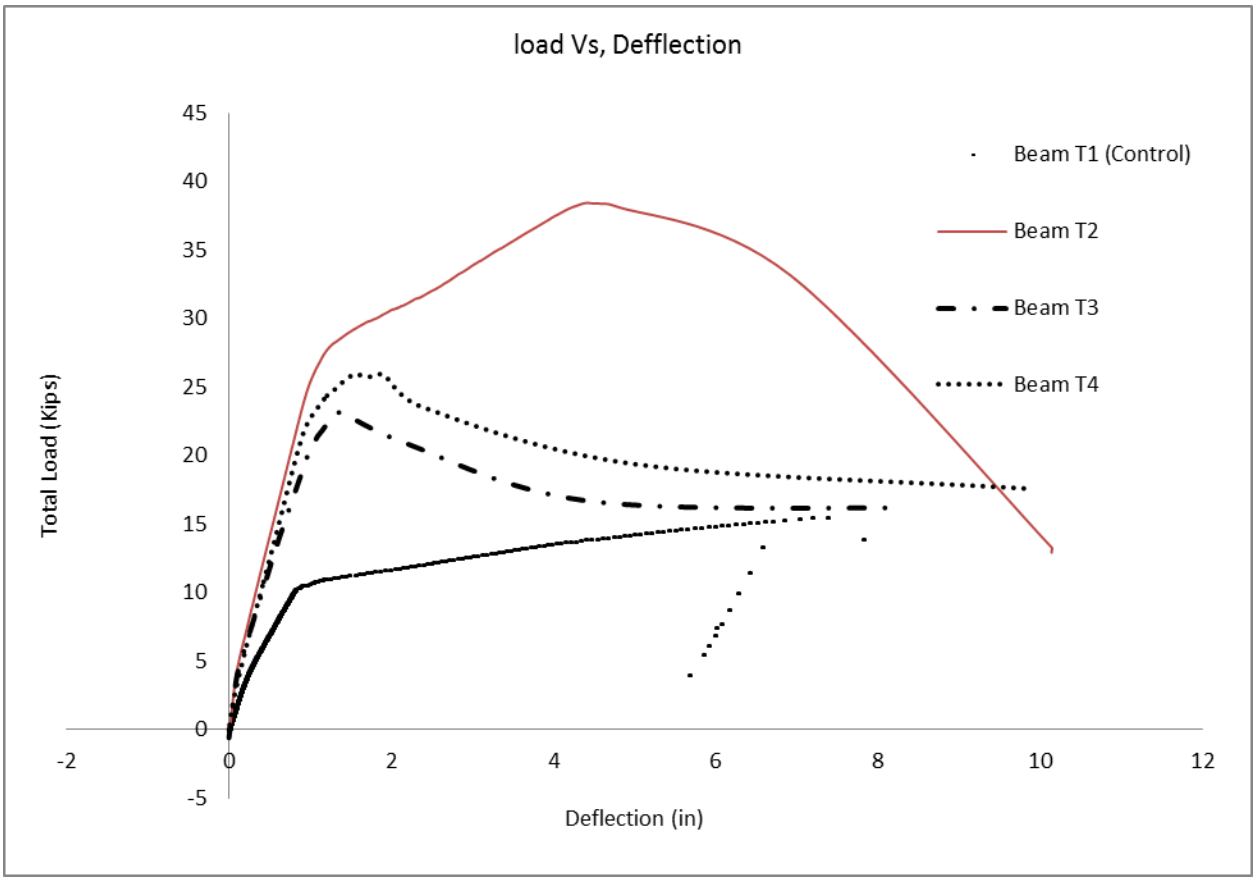

Figure 4-30: Comparison of Analytical and Experimental Load vs. Deflection for All Specimens.

CHAPTER 5. CONCLUSIONS AND RECOMMENDATIONS

5.1. Conclusions

The present experimental study is performed on the flexural behavior of reinforced concrete T-beams strengthened by a combination of GFRP composite laminates and NSM steel bars. Four reinforced concrete T-beams shaped having same reinforcement detailing were casted and tested. This research has approached its main goal. From the test results, the following conclusions can be summarized as follows:

- Using the combination of full length NSM bars and GFRP composite laminates was very effective. The ultimate load carrying capacity of all the strengthened beams was improved as compared to the Control Beam T1.
- The GFRP could sustain and confine the concrete cover at the tension region to postpone the cover delamination.
- The combination of full length NSM bars and GFRP composite laminates could approach an ultimate load capacity relatively high and resulted in an increase of about 249 % in capacity over the control beam.
- The development length of the 7.5 ft NSM steel reinforced beam was not enough and caused a relatively premature failure due to stress concentrations at the end of the of the NSM bars.
- Since that the GFRP sheets are relatively easier to install and less costly than some other materials such as CFRP, the use of combination of NSM steel bars and GFRP composite laminates may reduce the cost of strengthening.
- The use of GFRP sheets may isolate the concrete cover and make the structure more durable.
- The epoxy around the NSM rebars isolates the rebars from the deicing salt attack.
- Using the technique of combination between NSM steel bars and GFRP composite laminates could be an efficient way to repair concrete.
- Using the technique of combination between NSM steel bars and GFRP sheets is desirable because it provides more ductility in the failure mode.

5.2. Recommendations

The research posed few recommendations for future work. A research studying the effects of losing the bond between the concrete cover and GFRP because of an accident or a fire shall be considered. Although the study showed that the technique was successful at the accelerated short term, the very long term environmental effects still need to be studied. Other research should be conducted to evaluate the shear and torsion load capacity of the combination between NSM steel rebars and GFRP composite laminates. Finally, the use of U-wrapped GFRP at the end of short NSM steel bars is expected to delay the premature failure of the beam with short NSM rebars.

References

ACI Committee 440, 2008, Guide for the Design and Construction of Externally Bonded FRP Systems for Strengthening Concrete Structures (ACI 440.2R-08), American Concrete Institute, Farmington Hills, Mich., 76 pages.

Bournas, D.A. & Traintafillou, T.C. , 2008. Flexural strengthening of RC columns with near surface mounted FRP or stainless steel reinforcement: experimental investigation, The 14th World Conference on Earthquake Engineering, October12-17, 2008, Beijing, China, P2

Castro, E. K., Melo, G. S., and Nagato, Y., (2007) "Flexural Strengthening of RC T-beams With Near Surface Mounted (NSM) FRP Reinforcements," FRPRCS-8, University of Patras, Patras, Greece, July 16-18.

Chajes, M. J., Thomson, T., Finch, W. W., and Januszka, T. (1994), "Flexural strengthening of concrete beams using externally bonded composite materials," Construction and Building Materials, Vol.8, No. 3, pp.191-201.

Chajes, M.J.; Finch, W.W.Jr.; Januszka, T.F.; and Thomson, T.A. (1996). "Bond and Force Transfer of Composite Material Plates Bonded to Concrete", ACI Structural Journal, ACI, Vol. 93, No. 2, pp. 295-303.

Chen, J.F., Ye, L.P., Teng, J.G. and Rotter, J.M. (2005) "Flexural Trengthening Of Rc Beams Using Externally Bonded Frp Sheets Through Flexible Adhesive Bonding" Proceedings of the International Symposium on Bond Behavior of FRP in Structures (BBFS 2005).

Choi, H. T., (2008) "Flexural Behaviour of Partially Bonded CFRP Strengthened Concrete T-Beams," Ph.D Dissertation, University of Waterloo, Waterloo, Ontario, Canada.

Decker, B. R., (2007) "A Method of Strengthening Monitored Deficient Bridges," Masters Thesis, Department of Civil Engineering College of Engineering, Kansas State University, Manhattan, Kansas.

Dhinakaran, G., Manoharan, K., and Jeyasehar, C. A., "Load deformation characteristics of GFRP reinforced HPC square columns," Journal of Civil Engineering Research and Practice, Vol. 7 No.2, October 2010, pp. 23 – 38.

Fam, A. Z. and Rizkalla, S. H., "Flexural Behavior of Concrete-Filled Fiber-Reinforced Polymer Circular Tubes", ASCE Journal of Composites for Construction, Vol. 6, May 2002, pp.123-132.

GangaRao HVS, Vijay, P.V., Gupta, R., Barbero, E., and Damiani, T., 2001, " FRP Composites Applications for Non-Ductile Structural Systems: Short- and Long-Term Behavior," Report Submitted to (CEERD-CT-T)-US Army Corps of Engineers.

GangaRao HVS., Vijay, P.V, 2010, "Feasibility Review Of Frp Materials For Structural Applications," Report Submitted to (CEERD-CT-T)-US Army Corps of Engineers.

Grace, N. F., Soliman, A. K., Abdel-Sayed, G., and Saleh, K. R. (1999), "Strengthening of continuous beams using fiber reinforced polymer laminates," Proceedings of 4th International Symposium on Fiber Reinforced Polymer Reinforcements for Reinforced Concrete Structures, SP-188, American Concrete Institute, Farmington Hills, Michigan, USA, pp.647-657.

Hoy, D. E., Warren, G. E., and Davis, D. A. (1996), "Environmentally acceptable piling for use in Navy Pier Fender Systems," Proceeding of 4th ASCE Materials Conference on Materials for the new Millennium, November 1996, Washington, DC.

Kalluri, R. K. (1999), "Bending Behavior Of Concrete T-Beams Reinforced With Glass Fiber Reinforced Polymer (GFRP) Bars," Masters Thesis, West Virginia University.

Malek, A. M., Saadatmanesh, H., and Ehsani, M. R. (1998), "Prediction of failure load of R/C strengthened with FRP plate due to stress concentration at the plate end," ACI Structural Journal, Vol. 95, No. 1, pp. 142-152.

Meier, U., "Bridge Repair with High Performance Composite Materials", Material und Technik 15, 1987, 125–128 (in German and in French).

Rahimi, H., and Hutchinson, A. (2001), "Concrete Beams Strengthened with Externally Bonded FRP Plates," J. Compos. for Constr., ASCE, 5(1), pp. 44-56.

Rajamohan, S., and Sundarraja, C. M., (2008) "Strengthening of RC beams in shear using GFRP inclined strips – An experimental study," Construction and Building Materials, Vol. 23, 2009, pp. 856–864

Rasheed, H. A., Decker, B., Esmaeily, A., Peterman, R. J., Melhem, H., (2008), "Examining Transverse CFRP System to Develop the Flexural Capacity of CFRP Strengthened Beams," 3rd International Material Society Conference, Applications of Traditional and High

Performance Materials in Harsh Environment, International Material Society (IMS), American University of Sharjah, Sharjah, UAE, Jan. 23-24.

Rasheed, H.A., Harrison, R.R., Peterman, R.J. & Alkhrdaji, T., (2009), "Ductile Strengthening Using Externally Bonded and Near Surface Mounted Composite Systems. Composite Structures," Vol.92, No.10, (2010), pp. 2379-2390.

Rubinsky, I. A., and Rubinsky, A., (1954), "An investigation into the use of fiber-glass for prestressed concrete", Magazine of Concrete Research, Vol.6.

Shit, T., (2011) "Experimental And Numerical Study on Behavior of Externally Bonded RC T-Beams Using GFRP Composites," Masters Thesis, Department Of Civil Engineering National Institute Of Technology Rourkela, Orissa, India.

Sharif, A. M., Al-Sulaimani, G. J., Basunbul, I. A., Baluch, M. H., and Ghaleb, B. N. (1994), "Strengthening of Initially Loaded Reinforced Concrete Beams Using FRP Plates", ACI Struct. J., 91(2), pp. 160 -168.

Soliman, S.M., El-Salakawy, E., & Benmokrane, B., (2008), "Flexural Behavior Of Concrete Beams Strengthened With Near Surface Mounted FRP Bars," Fourth International Conference on FRP Composites in Civil Engineering (CICE2008), 22-24 July 2008, Zurich, Switzerland.

Soudki, K.A. (2000) "Behavior of Reinforced Concrete Beams Strengthened with Carbon Fiber Reinforced Polymer Laminates Subjected to Corrosion Damage." Canadian Journal of Civil Engineering 27, pp. 1005-1010.

Swamy, R. N. and Mukhopadhaya, P. (1999), "Debonding of Carbon Fiber Reinforced Polymer Plate from Concrete Beams", Proc. Instn Civ Engrs Structs & Buldgs, 134(4), pp. 301-317.

"V-Wrap Composite Strengthening System," PART I: Surface Repair & Preparation. S.l.: Structural Technologies, April 26, 2012.

"V-Wrap Composite Strengthening System, PART II: Installation of V-Wrap Sheet. S.l.: Structural Technologies, April 26, 2012.

Toutanji, H. and Ortiz, G. (1997) "Durability Characteristics of Concrete Beams Externally Bonded with FRP Composite Sheets." Cement and Concrete Composites Vol.19, No.4, pp. 351-358.

Wines, J. C., Dietz, R. T., Hawley, J. L., (1966), "Laboratory Investigation of Plastic-Glass Fiber Reinforcement for Reinforced and Prestressed Concrete," United States Army Crops. Of Engineers, WES, Vol. 1 & 2, Vicksburg, MS.

Appendix A – Materials Properties

- **Actual Beam Geometry of Each Beam at Midspan of the T shape:**

The compression strength of the used concrete is f'c = 8000 psi. Table A-1 shows the actual dimensions of each beam.

Table A-1: Actual Dimensions of Each Beam at Midspan.

Beam ID	d (in)	b_f (in)	h	h_f (in)	b_w (in)	Remarks
T1	10.50	16.0625	12.250	4.0000	6.0000	Control
T2	10.25	16.2500	12.250	3.9375	6.1250	Full Length
T3	10.50	16.1250	12.250	4.0000	5.8750	Short NSM for corrosion
T4	10.25	16.3125	12.188	4.0000	6.1875	Short NSM

- **Steel Properties:**

Figure A-1 shows the Stress-Strain curve of the tensile test of rebar that was performed at Kansas State construction lab according to ASTM A370 - 12a (Figure A-2). The results are shown in Table A-2.

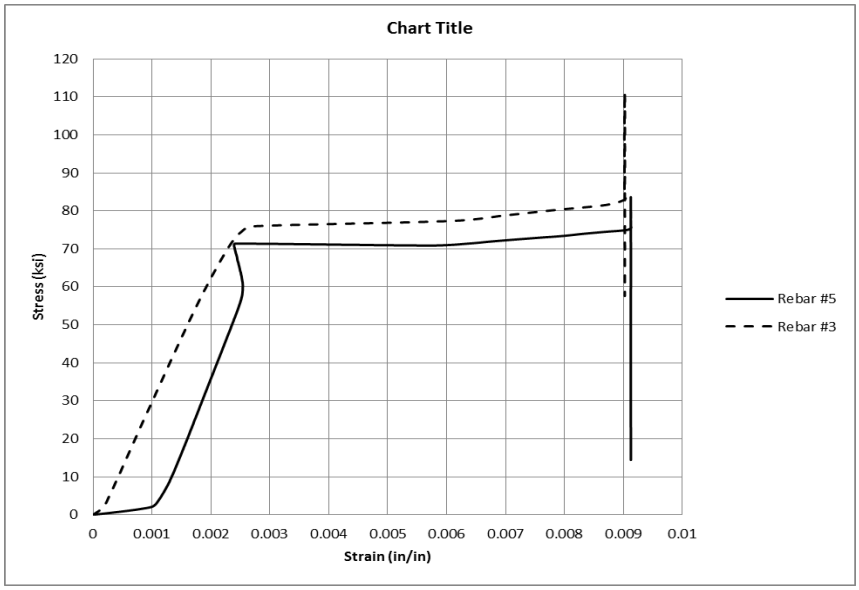

Figure A-1: Stress vs. Strain of steel rebars.

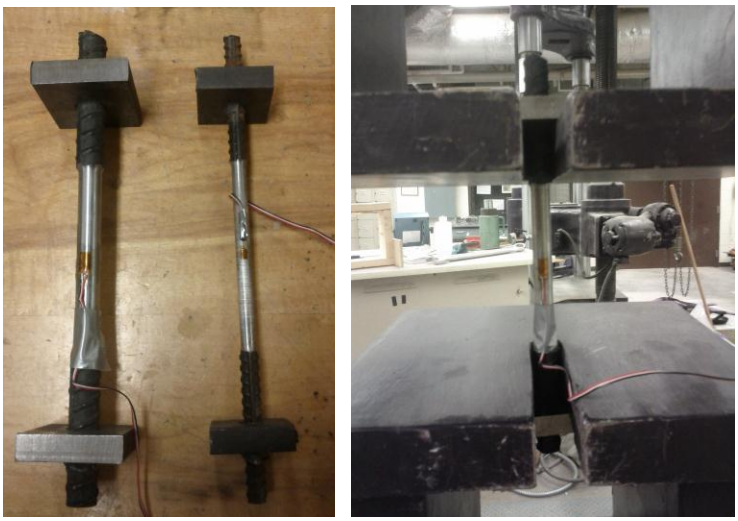

Figure A-2: Rebars Tensile Test According to ASTM A370 - 12a.

Table A-2: The Results of the Tensile Test of Rebars #3 and Rebars #5.

Rebar No.	Dimeter (in)	Modulus of Elastisty	Yield Stress fy (ksi)
#3	0.305	29000	75
#5	0.500	29000	71

- **GFRP Properties:**

The manufacturer cured laminate properties are provided by the producer (Table A-3). However, the cured laminate GFRP were tested according to ASTM D3039. Figure A-3 shows the Stress-Strain curve of the tensile test of GFRP composite laminates that was performed at Kansas State Mechanical Engineering lab. The actual measurements are shown in Table A-4 and the results are shown in Table A-5.

Table A-3: Manufacturer Cured Laminate Properties of GFRP

	Tensile Strength:	Modulus of Elasticity	Elongation at Break	Thickness	Strength per Inch Width
Average Value	83,400 psi	3.79 x 10^6 psi	2.2%	0.05 in	4,170 lbs/layer
Design Value	66,720 psi	3.03 x 10^6 psi	1.76%	0.05 in	2,660 lbs/layer

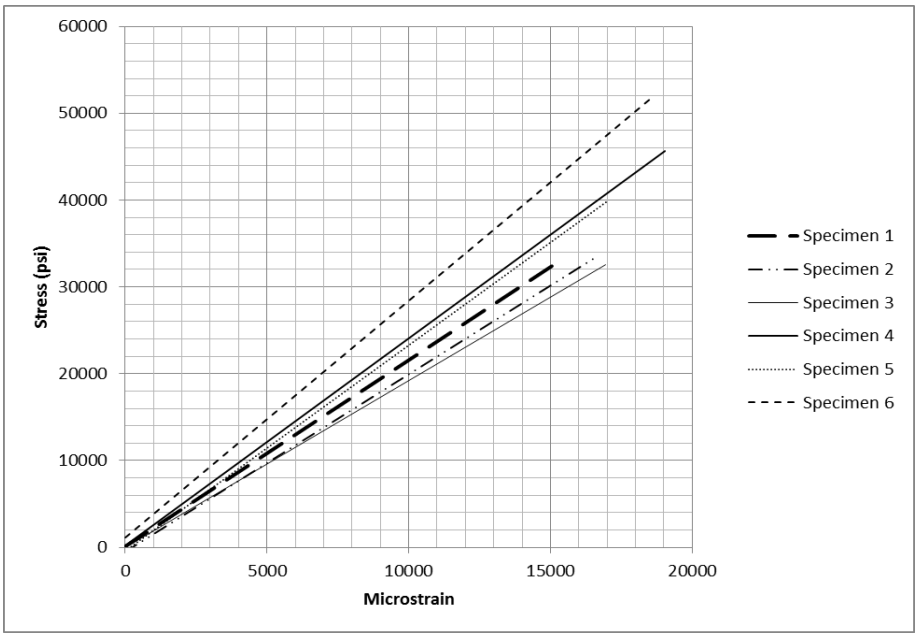

Figure A-3: Stress vs. Strain of GFRP Composite Laminates.

Table A-4: Dimensions of GFRP Specimens and Failure Load.

Coupon Specimen	Layers	Thickness 1 (in.)	Thickness 2 (in.)	Average Thickness (in.)	Width (in.)	Failure Load (lb)	Cross Sectional Area (in^2)
1	1	0.096	0.102	0.0990	1.0	3300	0.099
2	1	0.105	0.102	0.1035	1.0	3800	0.1035
3	1	0.112	0.110	0.1110	1.0	3550	0.111
4	2	0.162	0.170	0.1660	1.0	7450	0.166
5	2	0.141	0.143	0.1420	1.0	5465	0.142
6	2	0.152	0.151	0.1515	1.0	7600	0.1515

Table A-5: The Results of the Tensile Test of GFRP GFRP Composite Laminates.

Specimen	Width	Average Thickness	Ultimate Strength (ksi)	Modulus(ksi)	Ultimate Strain (με)
GFRP-1	1.00	0.099	32.7	2173	15065
GFRP-2	1.00	0.103	32.7	1971	16598
GFRP-3	1.00	0.111	31.9	1886	16936
GFRP-4	1.00	0.166	44.5	2026	21954
GFRP-5	1.00	0.142	38.5	2265	16987
GFRP-6	1.00	0.152	50.2	2688	18675
Average GFRP	-	-	38.4	2168	17702

Appendix B – Cyclic Load Procedure to Crack Beam T3

Figure B-1 below shows the cyclic load that was used to let the beam T3 crack in order to accelerate the corrosion process.

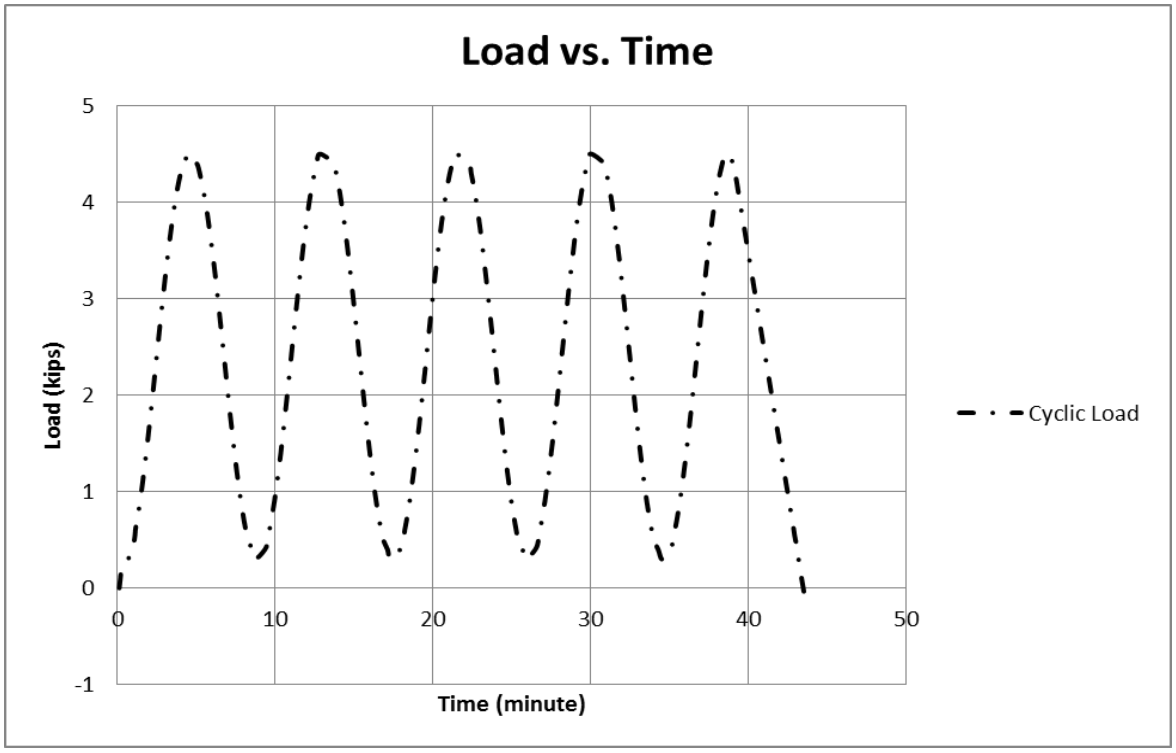

Figure B-1: Cyclic Load That Was Used to Let the Beam T3 Crack in Order to Accelerate the Corrosion Process.